Title:

High-power optical photovoltaic transmission: towards a new paradigm

Authors:

Pablo Sanmartín[1,*], Eduardo F. Fernández[1,**], Antonio García-Loureiro[2] and Florencia Almonacid[1]

Affiliations:

1 = Advances in Photovoltaic Technology (AdPVTech), CEACTEMA, University of Jaén, 23071 Jaén, Spain

2 = Department of Electronics and Computer Science, CITIUS, University of Santiago de Compostela, 15782 Santiago de Compostela, Spain

[*]Corresponding author: pandujar@ujaen.es, Tel. +34 953 213309

[**]Corresponding author: eduardo.fernandez@ujaen.es, Tel. +34 953 213520

Abstract:

High-power optical transmission (HPOT) holds transformative potential for revolutionizing energy delivery, offering a groundbreaking leap forward in how power is supplied and accessed. By utilizing a monochromatic light source as emitter and an optical photovoltaic converter as receiver, HPOT systems enable the sustainable transfer of kilowatts of power over hundreds of kilometers, overcoming the limitations of conventional copper wiring. This technology unlocks an extensive range of applications, from underwater environments to outer space, while driving disruptive advances in strategic fields such as energy supply, defense, communications, and healthcare. This work provides a comprehensive review of HPOT systems, including both optical wireless power transmissions and power-over-fiber systems. It begins with a historical overview and a description of the key performance indicators of the technology, followed by an evaluation of suitable high-power light sources. Then, the physical phenomena affecting light propagation are examined, as well as tracking mechanisms and safety measures that must be considered. Next, the photovoltaic receiver is analyzed in terms of intrinsic and extrinsic losses, and a comprehensive compilation of state-of-the-art performance results is presented. Finally, terrestrial and space prospective applications are explored, along with a survey of HPOT demonstrations conducted to date. Through a detailed research of the advantages, challenges, and key achievements of HPOT technology, this review aims to provide valuable insights to accelerate its development and adoption, paving the way for a more connected and sustainable future.

Keywords:

energy efficient usage, clean energy, high power optical transmission, optical wireless power transmission, power over fiber, light propagation, optical photovoltaic converters

Glossary

Nomenclature

c - Speed of light, m s^{-1}

C_n^2 - Refractive-index structure parameter, $m^{-2/3}$

d - Distance, m

E_g - Energy gap, eV

EQE - External quantum efficiency, %

FF - Fill factor, %

h - Planck constant, m^2kg s^{-1}

I - Electrical current, A

I_p - Peak intensity, W

$L_{i,j}$ - Additional losses
M^2 - Beam quality factor, dimensionless
n - refractive index, dimensionless
P_{in} - Input power, W
P_{out} - Output power, W
P_S - Light source power, W
RL - Radiative efficiency limit, %
R_S - Series resistance, Ωcm^{-2}
T - Temperature, K
T_C - Temperature coefficient, % K^{-1}
$v_\perp$ - Transverse fluid velocity, m s^{-1}
V_{mpp} - Voltage at the maximum power point, V
V_{OC} - Open-circuit voltage, V

Greek symbols
α - Absorption coefficient, m^{-1}
β - Scattering coefficient, m^{-1}
$\eta_{E\text{-}E}$ - End-to-end efficiency, %
$\eta_{E\text{-}O}$ - Electrical-to-optical efficiency, %
$\eta_{O\text{-}E}$ - Optical-to-electrical efficiency, %
η_{PV} - Photovoltaic efficiency, %
η_S - Light source efficiency, %
η_T - Transmission efficiency, %
Θ_D - Divergence due to diffraction, mrad
Θ_J - Divergence due to mechanical jitter, mrad
Θ_L - Divergence due to linear effects, mrad
Θ_Q - Divergence due to beam quality
Θ_S - Divergence or angular spread, mrad or degrees
Θ_T - Divergence due to turbulence, mrad
Θ_{TB} - Divergence due to thermal blooming, mrad
λ - Wavelength, nm
ρ_{in} - Input power density, Wcm^{-2}
τ - Extinction coefficient, m^{-1}

Abbreviations
AEL - Accessible Emission Limit
ANSI - American National Standards Institute
AUV - Autonomous underwater vehicle
CPV - Concentrator photovoltaics
CW - Continuous-wave
DCCPC - Dielectric-cross compound-parabolic-concentrator
DPAL - Diode-pumped alkali laser
DPSSL - Diode-pumped solid-state laser
ESA - European Space Agency
HPOT - High-power optical transmission
ICNIRP - International Commission on Non-Ionizing Radiation Protection
IEC - International Electrotechnical Commission
LD - Laser diode
LPC - Laser power converter
MJ - Multi-junction
MPE - Maximum Permissible Exposure

mrad - milliradian
NASA - National Aeronautics and Space Agency
NOHD - Nominal Ocular Hazard Distance
OPC - Optical photovoltaic converter
OWPT - Optical wireless power transmission
PCSEL - Photonic-crystal surface-emitting laser
PoF - Power-over-fiber
PPC - Photonic power converter
PV - Photovoltaic
PVLPC - Photovoltaic laser power converter
RTP - Refractive truncated pyramid
RL - Radiative limit
SBS - Stimulated Brillouin scattering
SBSP - Space-based solar power
SCL- Semiconductor laser
SILO - Single-lens-optical element
SPM - Self-phase modulation
SRS - Stimulated Raman scattering
SSL - Solid-state laser
UAV - Unmanned aerial vehicle
VCSEL - Vertical-cavity surface emitting laser
VECSEL - Vertical external-cavity surface emitting laser
WPT - Wireless power transmission
XPM - Cross-phase modulation

1. Introduction

Providing immediate, reliable energy anytime, anywhere is a challenge far from being trivial. Limited storage capacity, the absence of nearby power grids, environmental hazards, and physical constraints in conventional power delivery methods have historically made this issue particularly complex to resolve [1]. It is in these situations where high-power optical transmissions (HPOT) excel. Often referred to as power beaming or power-by-light [2], this technology consists in a monochromatic light source that transfers energy via optical beams to a photovoltaic (PV) receiver. By eliminating the constraints of traditional electrical cables, HPOT enables the transmission of kilowatts of power over distances in the order of tens of kilometers, or even further, and it also supplies energy in environments where traditional wires are problematic or impossible to use safely. In this sense, optical energy transmission provides unique advantages compared to electrical methods, such as operational flexibility, galvanic insulation, immunity to electromagnetic interference, elimination of electric sparks risks, weight reduction due to minimized cabling and energy storage, and the ability to simultaneously transfer both power and data [3–6]

In general, two main approaches within HPOT can be identified: optical wireless power transmissions (OWPT) [7], which are strictly cable-free, and transmissions through optical fibers, usually called power-over-fiber (PoF) [2,8]. Regarding the former, OWPT has been considered an expensive and inefficient alternative to existing technologies until recently [1], when these drawbacks have been progressively mitigated thanks to intensive research and development efforts, which has already provided a commercial-scale production and widespread adoption across industries of its key components.[1]. While efficiency improvements remain indeed necessary [9], that does not prevent the technology from enabling a vast variety of applications across both spatial and terrestrial (atmospheric and underwater) domains, with potential impact across multiple fields such as energy transmission, communications, defense, and even healthcare [10–13]. Optical transmissions offer versatile remote powering capabilities ranging from small

devices such as sensors and pacemakers, medium-size targets and vehicles like robots, rovers, and aircrafts, and extending to large-scale infrastructures, including uninterrupted energy supply from virtual space grids, such as space- and moon-based solar power stations [14–26]. This has positioned OWPT as one of the most promising far-field wireless power transmission (WPT) technologies [4], contributing to the remarkable growth of the wireless transmission market, valued at $13.3 billion in 2023 and projected to reach $37.7 billion by 2032 [27]. This growth is further evidenced by the recent emergence of numerous OWPT-based companies, which will be commented later.

Moreover, OWPT exhibits several benefits over alternative far-field wireless technologies, particularly microwaves, including reduced spreading, superior directionality, lower susceptibility to electromagnetic interference, longer transmission distances, and greater compactness and portability [12]. These characteristics result in more concentrated energy (reducing transmission times), smaller receiver apertures, enhanced equipment relocation mobility, lower cost per unit mass, and improved data protection security. However, microwaves have their own advantages, such as higher power capabilities, better resistance to weather conditions, and potentially slightly better system performance [3,14,28–31]. Ultimately, the choice between the two technologies depends on specific environmental conditions and application requirements.

On the other hand, fiber optics are becoming increasingly popular [8]. When compared to traditional copper wires, they offer significant advantages: lighter weight, smaller size, and insulation against galvanic contacts and electromagnetic noise [6]. These attributes make fiber optics an ideal solution for applications in confined spaces and high-risk environments, such as exclusion zones in refineries, mines, fuel tanks, and nuclear power plants, where the risk of fire or explosion is significant [2]. Additionally, optical fibers facilitate reliable, fast, and secure data transmission, making them particularly well-suited for hazardous settings and aircrafts navigation systems, for example [32,33]. In summary, HPOT systems offer extensive potential applications, with many possibilities yet to be explored.

This work aims to provide a comprehensive review of HPOT systems, presenting high-power OWPT while also addressing PoF. To provide some context, the review begins with a brief history and description of the technology, highlighting its key performance indicators. Next, potential high-power light source options are examined, outlining the properties that they should exhibit and the suitable types currently available or expected in the near future. The paper then describes the phenomena affecting optical energy propagation, including attenuation, turbulence, thermal blooming, beam divergence, peak intensity variation, and other effects related to propagation via optical fibers, as well as tracking mechanisms and safety measures. After that, the PV receiver, or optical photovoltaic converter (OPC), is described and analyzed in terms of both its intrinsic and extrinsic losses. Additionally, an extensive compilation of reported results is presented, comparing the efficiencies and power outputs achieved. To conclude, the terrestrial and space applications of HPOT systems are explored, and a survey of publicly available HPOT trials is presented, examining the current limitations that faces this technology in various environmental contexts. Our intention is to provide an in-depth overview of this technology, with insights into its advantages, areas of improvement, and important achievements to date.

2. History, description and key performance indicators of the technology

The foundations of HPOT technology were laid several decades ago, dating back to the late 1960s. Peter Glaser, a prominent reference figure in the field, along with the National Aeronautics and Space Agency (NASA), were the first to attempt to realize Isaac Asimov's futuristic concept of wireless power transfer in space, originally presented in 1941 in his science fiction story "Reason" [34]. While Glaser focused solely on microwave technology [35], NASA also explored optical sources, such as lasers, as an alternative way to transmit high powers. In their first reports and up

until the 2000s, NASA studied the feasibility of OWPT, mainly for space applications [25,36–41].

In parallel, during the late 1970s, another branch of HPOT, known as PoF, started to take shape [42]. PoF differentiated itself by removing the wireless feature of HPOT systems, instead transmitting power through optical fibers rather than through an open medium, such as space, air, or water [8]. Far from being a disadvantage, PoF systems are well-suited to different but equally relevant applications, which will be further discussed in section 6.

Despite its relatively long history, HPOT (encompasses both OWPT and PoF systems) has only recently gained significant momentum and has been successfully applied across a wide range of settings [1,2,7,8]. Evidence of the growing interest in this topic can be seen in academic research, as illustrated in Fig. 1, where the number of publications and congresses has shown a noticeable surge over the past decade. Moreover, not only reputed research centers, universities, and government agencies have contributed to the field, such as the Fraunhofer Institute for Solar Energy (Germany), Advances in Photovoltaic Technology-University of Jaén and Solar Energy Institute-Technical University of Madrid (Spain), University of Ottawa and University of Sherbrooke (Canada), Tokyo Institute of Technology and Japan Aerospace Exploration Agency (Japan), Ioffe Institute of St. Petersburg (Russia), NASA and National Renewable Energy Laboratory (USA), and the European Space Agency (ESA), to cite some, but also the private sector is committed to exploit the potential of this technology; several startups, such as PowerLight Technologies, Aquila, Volta Space Technologies, ORiS, SunCubes, and SkyGrids, have recently burst into the power beaming market, joining more established companies, like JDS Uniphase Corporation, AzurSpace, Broadcom, and Spectrolab, among others. As can be seen, the industrial ecosystem around HPOT systems is growing fast and the future looks bright.

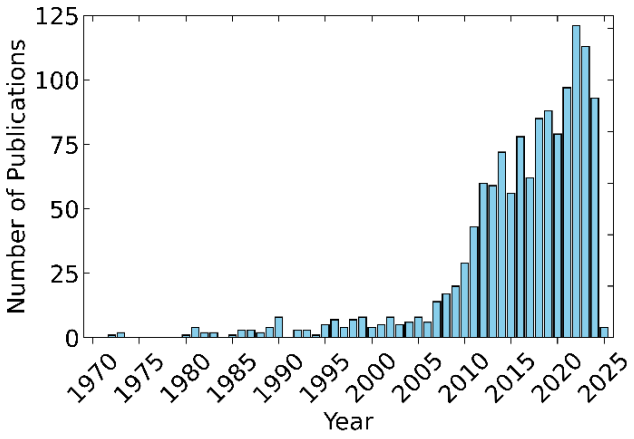

Fig. 1. Number of publications in relation to the HPOT topic [43].

The operation of HPOT systems involves delivering substantial energy to a remote device using a monochromatic (or quasi-monochromatic) light source. These systems are generally divided into two main sub-systems: the emitter and the receiver, as illustrated in Fig. 2 [2]. The emitter system includes a source that generates monochromatic light and ensures high-quality beam emission in terms of collimation, uniformity, and directionality, e.g. lasers. This requires equipment such as beam shaping and steering optics, a beam director, and power management and distribution electronics, which handle critical functions like thermal management, telemetry, safety, and tracking. The receiver system, in turn, consists of components that convert the transferred optical energy into electrical energy. The key component of this system is the PV receiver, referred to by various names, including optical photovoltaic converter (OPC), photonic power converter (PPC), photovoltaic laser power converter (PVLPC), or laser power converter (LPC), among others. For consistency, we will use the term OPC hereafter. Additionally, the receiver incorporates optics and control electronics similar to those used in the emitter system.

Regarding the transmission medium, the optical power can be transmitted either wirelessly through atmosphere, water, or vacuum (outer space), or via optical fiber cables. In all cases, traditional copper wiring is not involved in the transmission process.

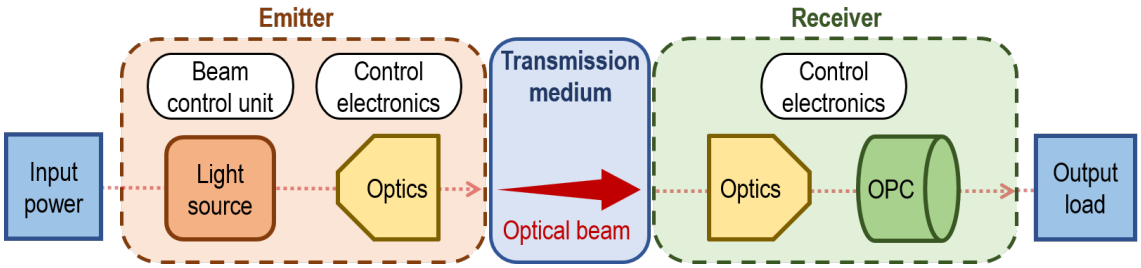

Fig. 2. Diagram of HPOT systems, illustrating the emitter and receiver sub-systems, from input to output power. The beam control unit consists of beam shaping and steering optics, as well as the beam director. The control electronics are the components that handle management and distribution tasks, including monitoring thermal sensors, telemetry, safety, and tracking equipment.

To evaluate HPOT systems, various indicators can be defined to quantify their performance and capabilities. Numerous parameters have been proposed, focusing on several aspects such as power, mass, area, volume, wavelength, time, and efficiencies across different parts of the system [1,44]. The most representative indicators from a general perspective are summarized in Table 1, and will be further discussed throughout the article.

Table 1. Key performance indicators of HPOT systems.

Indicator	Description
Electrical-to-optical efficiency ($\eta_{E\text{-}O}$)	Efficiency of the emitter system. Calculated as $\eta_{E\text{-}O} = \eta_S (1\text{-}L_i)$, where η_S is the efficiency of the light source, e.g. laser, and L_i accounts for the i-additional losses such as the optical losses from the optical emitting system, and the fraction of energy consumed by auxiliary components, including beam control electronics, sensors, wiring, tracking equipment, and other supporting elements. Units: %.
Transmission efficiency (η_T)	Ratio of input power at the receiver system to the output power from the emitter system. Units: %.
Optical-to-electrical efficiency ($\eta_{O\text{-}E}$)	Efficiency of the receiver system. Calculated as $\eta_{O\text{-}E} = \eta_{PV} (1\text{-}L_j)$, where η_{PV} is the PV efficiency of the OPCs, and L_j represents the j-additional losses such as the fraction of energy used by the control electronics and energy losses due to current mismatches among the electrical connection of several OPCs with an inherent electrical tolerance, optical losses from the optical receiving system to eventually spread and/or focused the light on the OPCs, and also due to light spillage, wiring, etc. Units: %.
End-to-end efficiency ($\eta_{E\text{-}E}$)	Overall system performance, calculated as the ratio of final output power to initial input power, or $\eta_{E\text{-}E} = \eta_{E\text{-}O} \times \eta_T \times \eta_{O\text{-}E}$. Units: %.
Power (P_S)	Optical power supplied by the light source. Units: W or kW. Alternative, it is sometimes given as power density: Wcm^{-2}.
Distance (d)	Spatial separation between the emitter and receiver systems. Units: m or km.
Divergence (Θ_S)	Angular spread of a beam as it propagates from the light source. It determines how far a beam can be effectively focused. Units: milliradians (mrad) or degrees.

These parameters provide a consistent basis for comparing not only HPOT systems but also extending to WPT systems, enabling the rapid identification of the most suitable configurations for the specific applications. Furthermore, they help pinpoint the components that most adversely affect overall performance and require attention. For instance, both electrical-to-optical and photovoltaic efficiencies are the areas where efficiency degradation is most significant, and further technological advancements are necessary to achieve more desirable system efficiencies [4].

3. Light source

As commented in the previous section, the emitter is a critical component of HPOT systems and one of the primary factors limiting the overall performance of the technology. Hence, selecting an appropriate light source is essential for high end-to-end efficiency ($\eta_{E\text{-}E}$). To accomplish this, the light source should exhibit the following characteristics [2,4,45]: (a) suitable wavelength (λ) for both PV conversion and light propagation; (b) high light source efficiency (η_S), enough power (ranging from watts to kilowatts depending on the application requirements), and continuous-wave (CW) mode operation is preferable over pulsed modes; (c) small beam divergence; and (d) good directionality and reliability.

Furthermore, it is advisable that the optical source demonstrates compactness, low weight-to-power ratio, low-cost, acceptable thermal management (avoid large cooling equipment, particularly in applications in which size and weight play a crucial role), long lifespan, stability, and, ideally, powered by sustainable sources. Bearing the above in mind, lasers emerge as clear candidates, as they can potentially fulfil all the aforementioned requirements [2,4,46–48].

Laser light possesses unique characteristics that distinguish it from other light sources: monochromaticity, coherence (temporal and spatial) and directionality [49]. These properties result in high radiance (also known as brightness, as it quantifies the power emitted per unit area per unit solid angle, measured in $Wm^{-2}sr^{-1}$), high spectral purity, variable repetition rate (from pulse to continuous wave), and excellent modulation control, making lasers ideal for high-power applications [45]. This section identifies the most suitable lasers for HPOT according to the aforementioned must-have characteristics.

- *Semiconductor lasers* (SCLs). SCLs use a semiconductor material as the active medium, achieving optical gain through stimulated emission from inter-band transitions at high carrier densities. Although technically solid-state devices, they are often classified separately due to their unique population inversion mechanisms [49]. The most common SCLs are *laser diodes* (LDs), electrically-pumped edge-emitting semiconductor lasers known for their high efficiency (~50%), compactness, acceptable cooling requirements, cost-effectiveness, and great modularity, as they are often stacked in arrays to increase output power [45–47,49]. LDs emit across a broad wavelength range, making them compatible with most PV materials. High-power LDs (up to 45 kW) are commercially available (e.g. QPC Laser, AeroDiode, Laserline [50–52]), but their low radiance requires advanced optical systems for compensation. Techniques like spectral beam combining can mitigate this limitation, but the achievable power level is considerably lower. Still, LDs are suitable for short-range power beaming (tens of kilometers) [46].

In addition to LDs, surface-emitting lasers such as *vertical-cavity surface-emitting lasers* (VCSELs) offer another approach. VCSELs emit light perpendicular to the wafer surface, enabling compact designs but with limited power output. To address this, *vertical external-cavity surface-emitting lasers* (VECSELs) incorporate external mirrors, improving power and beam quality and making them more suitable for high-power applications [49].

Despite the advantages of SCLs, their brightness remains a concern for its utilization in certain applications as the maximum values are around 100 $MWcm^{-2}sr^{-1}$ [53]. This has driven the development of *photonic-crystal surface-emitting lasers* (PCSELs), which incorporate a 2D photonic crystal to enhance performance. PCSELs achieve high single-mode coherent power, low

divergence, beam steering, polarization control, and superior beam quality [54–62]. Recent advancements include 50 W PCSELs achieving 1 $GWcm^{-2}sr^{-1}$ [63], with future goals targeting ~1 $TWcm^{-2}sr^{-1}$ brightness, ~10 kW power, and ~60% efficiency [53].

- *Diode-pumped solid-state lasers* (DPSSLs). DPSSLs are solid-state lasers optically pumped by LDs, ensuring a precise spectral overlap of the pump emission with the absorption band of the gain medium. While traditional optical excitation methods relied on lamp pumping or other laser types, LDs provide superior performance [64]. Their solid-state gain medium consists of crystals, glasses, or ceramics doped with rare earth or transition metal ions DPSSLs offer compact design, long lifespan, high efficiency, good and stable beam quality, and exceptionally high output power. The emission wavelengths span from 0.7 to 3 μm, although shorter values can be achieved in non-linear materials by frequency doubling methods [65–68].
Among solid-state lasers (SSLs), *fiber lasers* are particularly notable. They use rare earth doped fibers as active medium. Compared to bulk SSLs, fiber lasers exhibit higher efficiencies (up to 50% versus ~30% for bulk lasers, in exchange of requiring improved pumping LD), and a superior beam quality at more intense light output powers. They are robust, stable, and commercially available at 120 kW CW with >40% η_S (e.g. IPG Photonics [69]), making them a strong candidate for HPOT [49,70].
Disk lasers, another DPSSL variant, are characterized by a thin, circular shape. They deliver high power with acceptable beam quality (up to 24 kW CW [71]) and offer enhanced design flexibility and modularity for power scaling compared to fiber lasers [72,73], presenting a viable alternative for HPOT applications.

- *Diode-Pumped Alkali Lasers* (DPALs). DPALs are a recently developed class of gas lasers that use atomic alkali vapors as gain medium [74,75], offering excellent beam quality, reduced thermal issues, and outstanding scalability [76–78]. For instance, several demonstrations have reported, with one achieving a maximum power of 30 kW [79–81]. Theoretical studies suggest that DAPLs could scale to 100 kW while maintaining near diffraction-limited beam quality and excellent weight-to-power ratio, potentially outperforming DPSSLs and competing with fiber lasers for high-power CW applications [45,82]. Additionally, their emission wavelengths align with optimal absorption wavebands of main PV technologies, positioning DPALs as a promising option for laser power beaming [83].

As a summary, Table 2 presents the key characteristics for HPOT of the different types of lasers considered in this study.

Table 2. Typical performance parameters for high-power semiconductor lasers (SCL), diode-pumped solid-state lasers (DPSSL), and diode-pumped alkali lasers (DPAL). Max P_{out} stands for maximum output power, λ for wavelength, M^2 for beam quality, and $\eta_{E\text{-}O}$ for electrical-to-optical conversion efficiency. (*) Northrop Grumman 105.5 kW-laser achieved a beam quality of M^2 = 3 [84], while IPG Photonics reported a significantly higher M^2 = 140 for their 120 kW-laser [69]. (**) Estimated values.

Type of laser	Max P_{out} (kW)	λ (nm)	M^2	Weight-to-power ratio (kg kW^{-1})	$\eta_{E\text{-}O}$ (%)
SCL	~ 10 [52]	400 - 3000 [49]	~ 10 - 100 [52,85]	< 1 [85]	> 65 [86]
DPSSL	> 100 [69,84]	400 - 3000 [45]	~ 1 - 10 * [69,84]	> 20 [69]	> 40 [69]
DPAL	30 [81]	700 - 900 [83]	< 3 [87]	7 [82]	25 - 30 ** [83]

A special mention is given to *solar lasers*, as they represent a promising long-term alternative. Their operational principle relies on harnessing and concentrating sunlight to directly pump the

laser gain medium, usually a crystal or glass, although gaseous and liquid media are also used [88]. As a result, a coherent, collimated and monochromatic beam is obtained without requiring electrical or chemical power sources. This technology aligns with net-zero objectives, offering fully renewable energy delivery solutions, particularly interesting for space-based HPOT applications where powering the light source is challenging. However, significant improvements are needed to address current limitations, such as reducing device size, enabling operation at sunlight power density level, and increasing energy conversion efficiency, which remains below 10% [89]. Examples of lasers used in HPOT demonstrations are summarized in Table 3 (see section 6.3).

Beyond lasers, alternative solar-pumped techniques include sustainable quasi-monochromatic approaches such as luminescence solar concentrators [90] and holographic optical elements [91]. However, significant breakthroughs are required to make these technologies competitive with lasers. Future development efforts are justified as they enable sustainable HPOT systems.

4. Light propagation

Light transmission at high-power levels is complex, as photons can be significantly influenced by various phenomena upon emission, affecting both energy quality and quantity. These effects can critically impact system viability, making it essential to understand how environmental properties affect optical beams.

This section discusses key physical processes involved in high-power optical propagations, including attenuation and divergence, along with insights on tracking and safety measures. Other phenomena such as turbulence and thermal blooming are also briefly discussed. Given the early stage of the technology, this article primary focuses on atmospheric transmissions, as it represents the most convenient initial testing medium before advancing into more challenging scenarios, such as underwater. Nonetheless, it is important to note that in space applications some of the phenomena discussed in this work do not apply, since the propagation medium, i.e. vacuum, does not contain particles that could physically interact with light. Since transmission through optical fibers differs significantly from free space propagation, a dedicated section (section 4.4) is included to further address it.

4.1 Attenuation: absorption and scattering

Light beam propagation through non-vacuum media is affected by atoms, molecules, and aerosols, which absorb and scatter optical energy, reducing (attenuating) its power [92]. This combined effect is described by the extinction coefficient, $\tau(\lambda) = \alpha(\lambda) + \beta(\lambda)$, where α and β are the absorption and scattering contributions, respectively [93].

Attenuation characteristics vary significantly across media, as represented in Fig. 3. In water, attenuation is minimal near 450 nm but increases sharply at shorter and longer wavelengths [94,95]. In the case of the Earth's atmosphere, three different types of environments are considered (see Fig. 3): standard, considered the reference in the PV field; wet, corresponding to humid areas (water vapor = 4.11 cm); and hazy, related to extreme values of aerosols regions (aerosol optical depth at 500 nm = 0.5) [96]. However, their attenuation patterns are very similar: they slightly decrease with increasing wavelengths, although they exhibit some abrupt peaks due to absorption by atmospheric constituents such as CO_2, O_2, H_2O, aerosols, etc, and due to Rayleigh scattering at ultraviolet region. Additionally, it should be noted that weather conditions, such as fog or rain, further intensify atmospheric losses [45]. [96]Lastly, optical fiber (assumed fused silica) attenuation is dominated by Rayleigh scattering within the fiber below 1550 nm and by infrared absorption at longer wavelengths, with a notable peak at 1380 nm caused by OH^- impurity ion absorption from water dissolved in the glass [97].

Attenuation is strongly dependent on the photon wavelength. Therefore, it is crucial to select sources that fit the attenuation profile of the medium. Referring to Fig. 3, suitable propagation wavelengths for water fall within the 400 - 500 nm waveband, whereas for atmospheric

applications it would be advisable to avoid wavelengths in the vicinity of 950, 1150 and 1400 nm. Regarding optical fiber transmissions, three main transmission windows are usually considered, around 800, 1300 and 1550 nm [2].

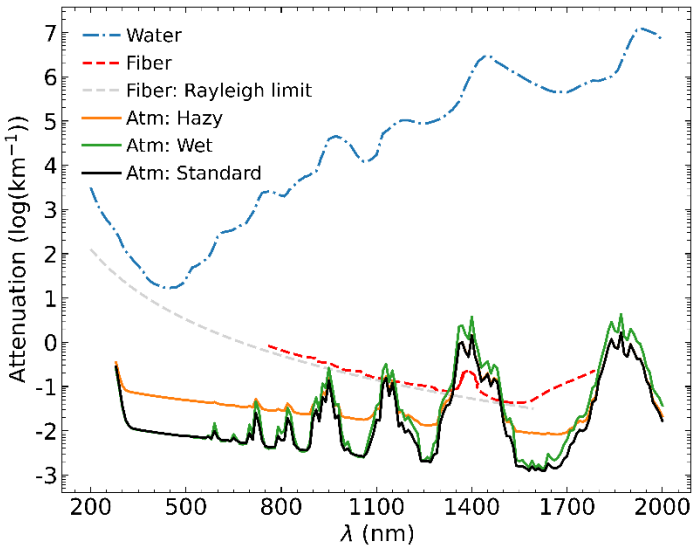

Fig. 3. Attenuation as a function of wavelength for water, optical fiber (assumed pure fused silica), and three types of atmospheres (denoted as "Atm"): standard, wet, and hazy. Rayleigh scattering attenuation in optical fiber was added to serve as a reference for ultraviolet transmissions in fiber optics. Refer to Ref. [96,98] for more information about water and atmosphere, and to Ref. [97] in the case of optical fiber.

Considering only attenuation losses, the optical input power (P_{in}) received by the OPCs can be estimated by means of the Beer-Lambert law [93,96,99]:

$$P_{in}(\lambda, d) = P_S \exp(-\tau(\lambda)d) \quad (1)$$

where P_S is the power emitted by the source, and d is the distance travelled by the beam. Note that τ includes the attenuation produced by all constituents of the medium. This serves as a first estimate in system design, subject to further analysis of additional phenomena.

4.2 Turbulence and thermal blooming

The OWPT system performance can be further compromised by other environmental phenomena, such as turbulence and thermal blooming. Turbulence arises from random refractive index (n) fluctuations in the propagation medium, primarily due to temperature gradients, and, in seawater, also due to salinity and dissipation rates [45,100]. It causes effects like scintillation, beam wander, and beam spread, which deteriorates the beam shape and the intensity, as shown in Fig. 4. In strong turbulence conditions (refractive-index structure parameter $C_n^2 > 10^{-13}$ m$^{-2/3}$), loss of coherence and beam breakup can occur. Mitigation strategies include aperture averaging and adaptive optics, and using longer wavelengths due to the inversely proportional relationship [93,101].

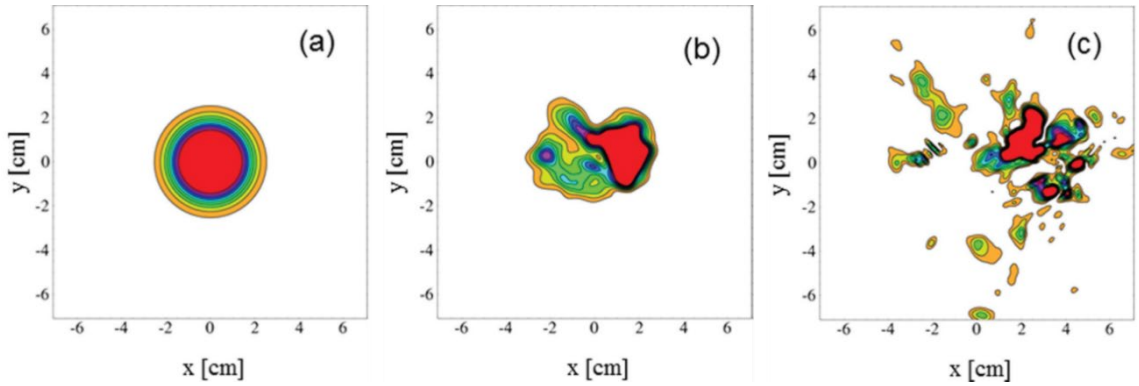

Fig. 4. Intensity contours at the target plane for three levels of turbulence depending on constant refractive-index structure parameter (C_n^2): a) no turbulence ($C_n^2 = 0$), b) moderate ($C_n^2 = 10^{-14}$ $m^{-2/3}$), and c) strong ($C_n^2 = 10^{-13}$ $m^{-2/3}$). Image adapted from Ref. [102].

Thermal blooming, on the other hand, is a nonlinear optical effect caused by the absorption of a high-power laser energy by the medium, leading to localized heating and variations in n. This results in an expansion of the beam diameter, a reduction in I_p, and, in the presence of a transverse current, an off-target displacement, as illustrated in Fig. 5 [103–106]. This phenomenon can seriously compromise the performance of HPOT systems: in the atmosphere, thermal blooming becomes a concern for transmission distances of several kilometers and power levels in the range of hundreds of kilowatts [93], whereas in underwater environments, its impact is expected to be substantially more severe [104,107]. Mitigation strategies, such as medium vaporization, beam rotation, and closed-loop adaptive optics, can help reduce its effects [108,109].

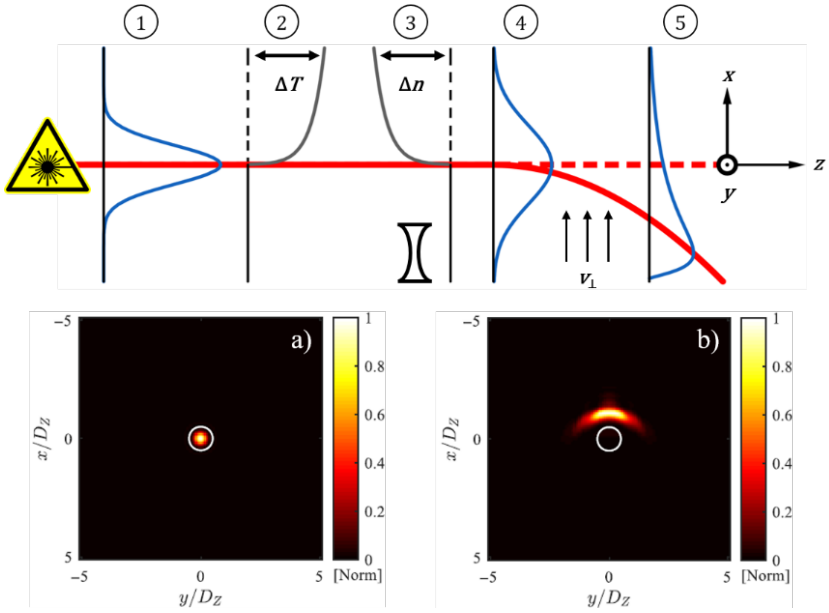

Fig. 5. Thermal blooming effect: considering a Gaussian beam propagating in z direction (1), the absorption of energy by particles of the medium heats the surrounding environment (ΔT) (2), resulting in a negative refractive index gradient (Δn) (3). The fluctuations of n act as divergent lenses, causing the beam to defocus, leading to an intensity reduction and a transverse scattering of the contour of the beam (xy-plane) (4). In the presence of fluid (air or water) flowing in the x-axis direction ($v_\perp$), the beam would deviate towards the opposite direction ($-x$) (5). The change in the beam profile is illustrated in the lower graphs, adapted from Ref. [103]: a) the diffraction-limited case in the absence of thermal blooming, and b) the steady-state thermal blooming case with a transverse flow. The white circle represents the diffraction limit contour.

4.3 Beam divergence and peak intensity

Beam divergence is a critical parameter for long-distance HPOT, as it broadens the beam diameter as it propagates, potentially leading to spillage losses. Divergence must be minimized to obtain a beam spot compact enough for its integration in the desired target, especially for small ones such as drones or rovers, ensuring efficient energy transfer to the remote system, while also reducing weight, non-uniformity effects, and costs.

The received beam profile results from the combination of multiple factors, including wavelength, beam quality, and source aperture, as well as environmental and mechanical influences such as turbulence, thermal blooming, and mechanical jitter caused by system motion or vibrations from cooling mechanisms and wind loads, for example [46,47,110]. These phenomena can interact synergistically or counteract, complicating divergence estimation. For simplicity, divergence is modeled here for a basic atmospheric case, assuming a Gaussian beam profile. The total divergence or angular spread (Θ_S) of a beam can be expressed as a combination of linear (Θ_L) and non-linear effects, consisting solely of thermal blooming (Θ_{TB}) in this particular case (for further insights, see Ref. [111,112]):

$$\Theta_S^2 = \Theta_L^2 + \Theta_{TB}^2 \tag{2}$$

The linear term (Θ_L) includes diffraction (Θ_D), turbulence (Θ_T), and jitter (Θ_J). Simplifying for uniform beams, zero slew rate, and horizontal propagation with a constant C_n^2, it can be expressed as:

$$\Theta_L^2 = \Theta_D^2 + \Theta_T^2 + \Theta_J^2 \tag{3}$$

For multi-mode lasers, the influence of beam quality (M^2) in its divergence is significant. For instance, it is considered to be more impactful than other linear effects, such as turbulence and diffraction [93]. Therefore, an additional term Θ_Q should be added to equation (3) when using lasers of higher-order modes:

$$\Theta_Q^2 = (M^2 - 1)\,\Theta_D^2 \tag{4}$$

Finally, it is possible to estimate the peak intensity (I_p) received at a distance d as [111,112]:

$$I_p(\lambda, d) = (P_S \exp(-\tau(\lambda)d))/(\pi d^2 \Theta_S^2) \tag{5}$$

where the numerator corresponds to the attenuated power as defined in equation (1), and the denominator corresponds the area at the receiver for a far-field fundamental transverse electromagnetic mode Gaussian beam with divergence angle Θ_S [113]. Prior to this formulation, Gebhardt [110] derived an empirical model accounting for both linear and non-linear detrimental effects. The analytical fit indicates that, although the peak irradiance increases with P_S, at some point, the heating produces a blooming of the beam area that overshadows the effect of the increased power, leading to a counterintuitive decline in light intensity as power rises. This curve is commonly called the power optimization curve. Other authors also state that strong turbulence can cause a similar effect [93].

4.4 Optical fiber

Optical fibers can only transmit up to a certain power level before experiencing physical damage or reduced functionality. If this limit is surpassed, some detrimental phenomena may arise. One of the most impactful effects is the so-called fiber fuse, which is characterized by the formation of a visible bright spot of white light, considered to be plasma due to the estimated high temperature (5000-10000 K) associated with the spectrum of the emitted light, that propagates by

thermal diffusion towards the origin of the light source at an approximate velocity of 1 m s^{-1}, leaving behind a bubble-shaped track of irreversible and catastrophic degradation on the optical fiber core [114,115]. According to empirical observations [114,115], the power density threshold for fiber fuse is in the order of $MWcm^{-2}$, and it is dependent on the fiber composition and laser light wavelength.

However, solely exceeding the optical power threshold is insufficient to trigger the fiber fuse effect. A localized high-temperature ignition point is also required. The origin of this localized heating may come from different sources, such as from the energy leakage from the fiber core to the cladding due to an excessive bending of the optical fiber cable (which can be a problem on its own, as it can directly catch on fire), or from the absorption of the intense optical energy by contaminated or degraded connectors within the fiber [116].

Besides fiber fuse, non-linear effects may also occur at high-power optical densities, such as stimulated Brillouin and Raman scattering (SBS and SRS, respectively). These scattering phenomena originate from the interaction of light with acoustic (SBS) and optical phonons (SRS), and the intensity of the scattered light scales exponentially once the power threshold is exceeded [117]. While light waves scattered under SBS propagates backwards, downshifting the frequency several GHz, SRS can occur in both directions, changing the frequency of the scattered light in the order of THz [118]. Additionally, other non-linear effects may also appear, such as self-phase modulation (SPM) and cross-phase modulation (XPM). SPM is characterized by a phase shift of the optical signal produced by a refractive index variation induced by the high-power optical signal itself, whereas XPM occurs when multiple optical signals propagating through the same fiber mutually alter their phases due to the fiber non-linear refractive index [119].

There are multiple fiber types suitable for PoF applications (Fig. 6) [120]. Single-mode fibers offer low loss (0.2 $dBkm^{-1}$ at 1550 nm) for long distances but face power density limitations due to its small core. Conversely, multimode fibers can transmit higher powers due to its bigger core (diameter ranges from 62.5 to 200 μm), although simultaneous data transfer may be limited due to modal dispersion and crosstalk. In cases where the target is the simultaneous information and power transmission, specialized fibers like multicore fibers and double-clad fibers are the best options, where the latter stands out for its enhanced high-power transfer capabilities. In this context, hollow-core photonic crystal fibers and microstructured optical fibers are promising solutions. Hollow-core photonic crystal fibers achieve ultra-low non-linearity and tolerance to high powers in exchange of higher attenuation compared to silica fibers, whereas microstructured optical fibers exhibit enhanced power thresholds in comparison to conventional fibers. In conclusion, each architecture presents unique tradeoffs between power handling, data capacity, and transmission efficiency.

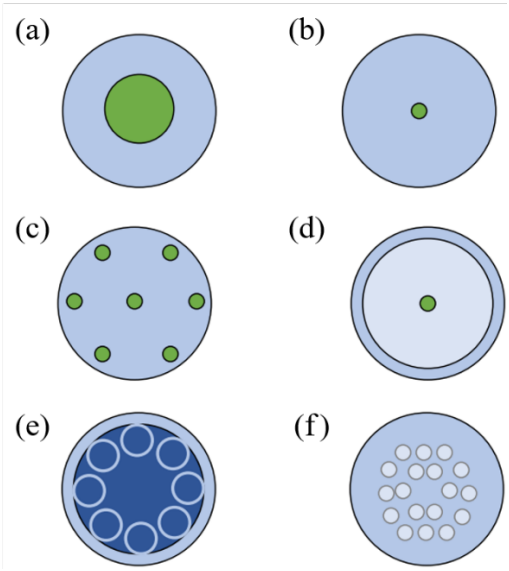

Fig. 6. Cross sections of various types of optical fibers. (a) Single-mode fiber, (b) multimode fiber, (c) multicore fiber, (d) double-clad fiber, (e) hollow-core photonic crystal fiber, (f) microstuctured optical fiber. Image from Ref. [120].

4.5 Tracking and safety

The operation flexibility provided by OWPT is both a remarkable feature and a complex challenge. This section briefly addresses tracking and safety considerations, which may initially be overlooked.

Efforts to minimize propagation losses and optimize the PV components of the system are useless if the beam is not accurately pointed at the target. A beam control system (illustrated in Fig. 7), is recommended to ensure precise aiming and sustained alignment for tasks such as recharging batteries or powering devices [49]. Typically, such systems consist of target-alerting and tracking mechanisms, a system processor, a gimbal-control system for beam stability, an accurate pointing mechanism, inertial sensors, a power supply, and an environmental protective cover. In dynamic applications, aero-optical effects from fluid flow over the emitter induce turbulence and refraction, reducing precision. Proper positioning of the beam director can mitigate these effects [45].

Fig. 7. Example of a high-power laser beam direction system for directed-energy applications [121].

In static configurations, beam alignment is relatively simple, but motion significantly complicates the challenge. Solutions vary depending on pointing requirements. Autonomous beam trackers

have successfully powered moving targets [122–125], while simpler GPS-based and manual tracking systems have also been developed [20,126].

Given the high source power densities involved, implementing safety measures is crucial, particularly in populated atmospheric environments where accidental exposure could cause severe injuries, including skin burns and retinal damage, or, in extremely rare cases, life-threatening hazards like skin cancer or electrocution risks (from power supply unit failures) [45,127]. International safety standards to regulate laser hazards and protective measures have been set by the International Electrotechnical Commission (IEC): "IEC 60825 Series" [128]. These norms are further implemented in national regulations; for example, the American National Standards Institute (ANSI) standard series ANSI Z136 [129].

Three key safety parameters are considered: the Accessible Emission Limit (AEL), the Maximum Permissible Exposure (MPE), and the Nominal Ocular Hazard Distance (NOHD). Whereas the AEL defines the maximum accessible emission level and serves as the basis for laser classification, the NOHD represents the distance from the source at which radiation levels equal the MPE. Among the different safety parameters, the MPE is the most relevant in the context of this article, as it determines the maximum irradiance level the main organs at risk (eyes and skin) can be exposed to without suffering short or long-term damage, according to International Commission on Non-Ionizing Radiation Protection (ICNIRP) [130]. Visible and near-infrared wavelengths pose the greatest risk to vision, as retinal focusing amplifies power density roughly by a factor of 10^5 [131,132]. Fig. 8 shows the MPE variations with exposure time for various wavelengths per IEC 60825. Ultraviolet A (315 - 400 nm) and long-infrared wavebands are considered less harmful for exposure times of up to approximately 100 s. It is worth mentioning that the safety response time to shut off the beam is around 1 ms, allowing more powerful laser to be safely used within these wavebands [133]. Regarding skin hazards, the damage is more severe at shorter wavelengths, particularly injurious within the ultraviolet B range (280 – 315 nm). Nonetheless, the hazards associated with skin exposure are of less importance than those for the eyes [127,134,135].

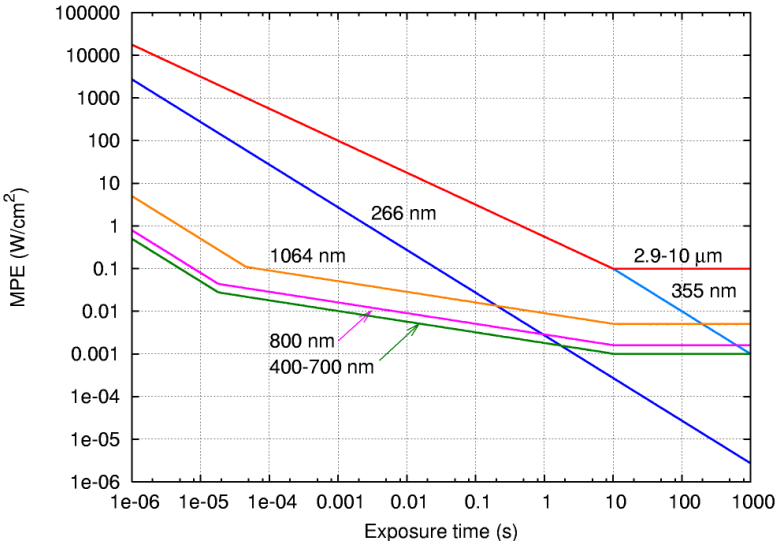

Fig. 8. Maximum permissible exposure (MPE) in Wcm^{-2} versus exposure time for various wavelengths based on IEC 60825 (Hankwang at English Wikipedia, via Wikimedia Commons [136]).

Several strategies to address the safety concerns have been proposed. Wi-Charge and Tongji University researchers developed a resonant cavity-based system that maintains power within MPE limits [137–140]. PowerLight Technologies' light curtain ensures that no obstacle is present along the beam propagation path by coaxially coupling a harmless beam with the primary laser

[9,141], similar to Washington University researchers' approach [16], and Aquila's three-tier lock system [142].. Other ideas based on advanced vision to detect objects entering a predefined safety zone and adjust P_S accordingly have also been developed [143].

5. Optical photovoltaic converters

Despite its origins dating back to 1977 [144], OPCs remain at critical bottleneck in advancing of HPOT technology [2,4]. This section outlines the fundamentals of OPCs, including their operating principles, primary loss mechanisms, and mitigation strategies, along with a comprehensive review of reported OPCs in the literature.

5.1 Ideal OPCs and intrinsic losses

OPCs are essentially PV cells optimized to efficiently convert monochromatic light into electricity. Ideally, illuminating a semiconductor with a wavelength matching its energy gap (E_g) would ensure complete photon collection without energy loss, as each photon provides precisely the energy needed to excite an electron into the conduction band. Unfortunately, this ideal scenario is unattainable in practice due to both intrinsic and extrinsic losses.

Intrinsic losses arise from unavoidable recombination processes during photovoltaic conversion. A thermodynamic analysis reveals that, under radiative recombination, the entropic losses from the absorption and emission of radiation are by far the dominant intrinsic loss mechanism [145]. However, these entropic losses can be significantly reduced by using wider bandgap semiconductors and increasing irradiance. These results are supported by similar studies in which the maximum theoretical efficiency for monochromatic illumination is calculated based on the radiative efficiency limit (also known as detailed balance limit or Shockley-Queisser limit [146]) [96,147]. As represented in Fig. 8 (left), for a constant input power density (ρ_{in} = 100 Wcm^{-2}), the PV conversion efficiency (η_{PV}) improves with increasing E_g. This is primarily due to an enhancement in the fill factor (FF): higher E_g reduce intrinsic losses, and, as a consequence, the voltage at the maximum power point (V_{mpp}) shifts closer to the open-circuit voltage (V_{OC}), pushing the FF towards unity (Fig. 9, right). A similar effect occurs with increasing illumination, which is one of the key phenomena used in concentrator photovoltaics (CPV) to obtain superior efficiencies compared to standard non-concentrator PV technologies [148–150].

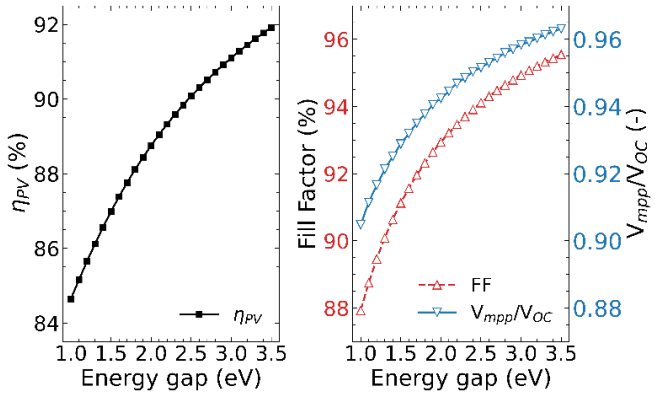

Fig. 9. Theoretical radiative photovoltaic efficiency (η_{PV}) limit (left), and fill factor (FF) and the ratio of the voltage at the maximum power point (V_{mpp}) and open-circuit voltage (V_{OC}) (right) as a function of energy gap. Assumptions: ideal photon absorption, external quantum efficiency (EQE) of 100%, temperature of 298 K, and energy gap equal to hc/λ, being h the Planck constant and c the speed of light. Note: since this section exclusively considers intrinsic losses, resistive losses are neglected for now, but they will be addressed in the next section.

Intrinsic losses also include other recombination mechanisms of non-radiative nature, such as Auger, defect-assisted, and surface recombination. While Auger recombination has minimal

impact on direct-band semiconductors unless carrier concentrations are extremely high [145,151–153], it represents a concern for indirect-band semiconductors, such as silicon [153,154]. These losses can be reduced by implementing textured surfaces, and spectral and angular filters which enhance light absorption, effectively equivalent to increasing incident irradiance, thereby improving efficiency [145]. On the other hand, recombination through defect traps or impurities can degrade device performance [155–157]. Growth complexities in some materials introduce structural defects that act as recombination centers. The associated losses can be reduced by improving the semiconductor quality through advanced growth techniques [158–160].

5.2 Extrinsic losses and mitigation strategies

In practical scenarios, extrinsic losses are inevitable. This section provides an overview of the primary sources of extrinsic losses, emphasizing the key challenges OPCs must overcome to achieve high efficiencies.

- *Series resistance*. PV cells exhibit parasitic series resistance (R_S) due to the inherent opposition of materials to charge carrier flow. This resistance arises from several physical mechanisms, with the primary contributors being the bulk resistance of the semiconductor material, the resistance of metallic contacts, and the resistance of the metal-semiconductor interface [151]. Its negative impact on device performance becomes a major concern at high ρ_{in}, as the associated power losses scale quadratically with current as I^2R_S. As a result, efficiency tends to increase logarithmically with irradiance until the effect of R_S takes over, drastically worsening device performance thereafter [2,96,98].

The impact of R_S in the performance of the OPCs is illustrated in Fig. 10, where the theoretical radiative efficiency limit is calculated for materials with low (1.0 eV) and high (3.0 eV) E_g. Two scenarios are considered: an ideal case ($R_S = 0$ Ωcm^{-2}) and realistic case ($R_S = 10^{-3}$ Ωcm^{-2}). The results show that as ρ_{in} exceeds the 100 Wcm^{-2} threshold, R_S losses become increasingly significant, particularly for the lower bandgap material, where the η_{PV} deviates substantially from the ideal projection (dashed line). The reason behind it is that, for a fixed ρ_{in} and assuming high energy gap materials are illuminated with shorter wavelength light beams, wider bandgap semiconductors receive fewer (but more energetic) photons than narrower bandgap materials, according to Einstein's photoelectric law. Consequently, the photogenerated current is inherently lower in wider bandgap OPCs, ultimately reducing their R_S losses [96].

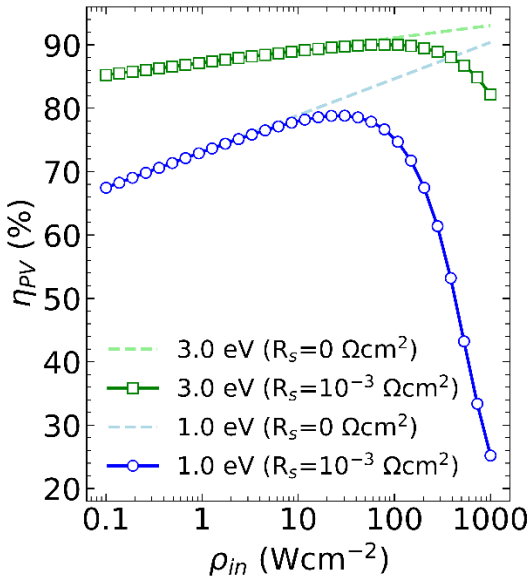

Fig. 10. Photovoltaic efficiency (η_{PV}) of low- (1.0 eV, blue) and high- (3.0 eV, green) energy gap materials, considering an ideal ($R_S = 0$ Ωcm^{-2}, dashed lines) and a realistic ($R_S = 10^{-3}$ Ωcm^{-2}, solid lines with markers) scenario of series resistance values (assumptions described in Fig. 9).

R_S is considered the main limiting factor of η_{PV} at high irradiances. Taking this into account, there are several approaches to mitigate its severe detrimental impact. One option focuses on cell architecture, where two types of structures can be signaled (see Fig. 11): horizontal, light falls on the top surface of the cell normal to the n-p junction plane; and vertical (also known as edge-illuminated), the device is illuminated parallelly to the n-p junction plane. In both configurations, it is possible to manufacture multi-junction (MJ) structures where each subcell can be interconnected in series either vertically or horizontally.

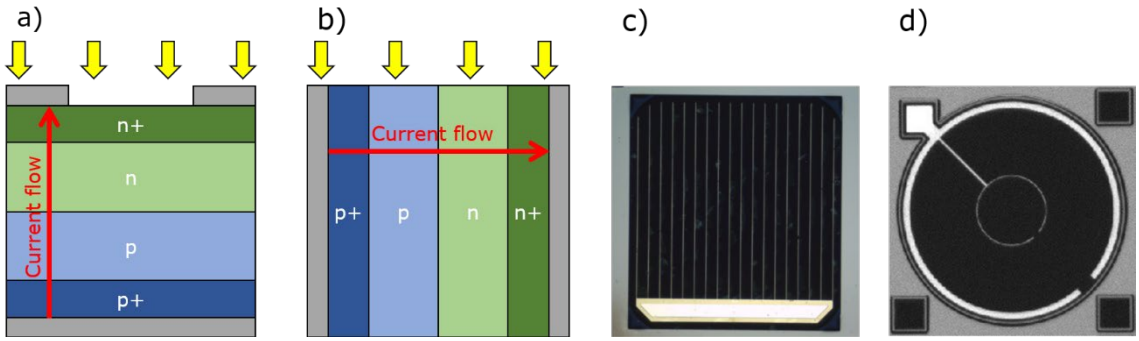

Fig. 11. a) and b) schematically illustrate horizontal and vertical n-p homojunction OPCs, respectively. Yellow arrows indicate the direction of incident illumination and metal contacts are represented in grey color. n and p represent the doping type of the layers, with the + sign denoting high doping concentration. Pictures c) and d) show different shapes and grid configuration examples of front surfaces of vertical architectures.

Considering horizontal structures, the front contact grid should be optimized according to the expected ρ_{in} and semiconductor bandgap, adjusting the pattern, width and spacing of the metallic fingers [161,162]. This architecture particularly benefits from a MJ approach, since it reduces R_S losses by splitting the total current across its multiple subcells. [161,162]Moreover, including a transparent heavily-doped lateral conduction layer on top of the window layer mitigates R_S impact, since it ultimately increases the lateral conductivity and collection of majority carriers [163].

Vertical architectures, on the other hand, offer advantages such as the mitigation of R_S losses due to the large cross-sectional contact area available for current flow, as the metal electrodes are located laterally. Also, this configuration allows for a drastic reduction of the current density due to the orthogonal incidence of the light on the p-n junctions and the current flow [164,165]. In this sense, vertical structures reduce device internal resistance and eliminates the trade-off between R_S and front contact shadowing [166,167]. The main issue lies in achieving sufficiently large areas for optical energy harvesting. Currently, the most promising solution involves the use of MJ structures connected via tunnel junctions [164,165]. The manufacture of this structure, however, is still challenging due to technical limitations, although there are some examples in the literature regarding its feasibility [168,169].

Material selection also plays an important role. Wider bandgap semiconductors require fewer but more energetic photons to collect the same energy as narrower bandgap semiconductors, resulting in less photogenerated current, thereby reducing R_S losses [96,98,163]. Additionally, thermal annealing techniques mitigates R_S losses by enhancing electrodes ohmic contact [170]. Nevertheless, this process must be carefully optimized to prevent degrade contact quality or accelerate device degradation. Precise control of temperature, duration, and ambient conditions is essential to achieve optimal ohmic contacts while minimizing adverse effects [171].

- *Beam non-uniformity*. Non-uniform illumination frequently occurs in HPOT, as non-flat-top Gaussian profiles are the most typical laser beam profiles. These non-uniform irradiance

distributions deteriorate OPC performance, particularly reducing the *FF* and V_{OC} [172,173]. Moreover, localized peak irradiances lead to lateral current spreading and current overdriving in certain areas of the front surface, increasing resistive losses [174–176]. The impact is considerably more severe in horizontally connected horizontal structures, also called multi-segment, where the photocurrent is limited by the subcell producing the lowest current, resulting in significant mismatch losses [177]. In contrast, vertically stacked monolithic MJ OPCs are less affected by non-uniformities, as the lower current flowing through each subcell mitigates the associated R_S losses. A potential drawback worth to mention of these structures is that their performance can be degraded if the peak current density of the tunnel junctions is exceeded, which could happen in rare cases of intense non-uniform irradiance [172,178]. In practice, nowadays, the peak current density of well-engineered state-of-the-art tunnel junctions (several thousands of Acm^{-2} [178–181]) has proven to not represent a limiting factor for most mature materials[182], since the R_S losses would impact the OPC's performance before reaching those intense power densities [183].

Non-uniformity losses can be minimized by optimizing the grid design to balances the trade-off between power losses from metal contact shadowing and from non-uniform illumination [172]. An alternative approach to achieve uniform illumination is the use of spherical enclosed receivers called powerspheres [184,185]. Additionally, drawing on the experience of the scientific community in the field of CPV, another potential strategy could involve homogenizers, such as dielectric-cross compound-parabolic-concentrator (DCCPC), single-lens-optical element (SILO-Pyramid) or refractive truncated pyramid (RTP) [186]. To the best of the authors' knowledge, these approaches have not yet been applied in HPOT. Based on the author's CPV experience, implementing these elements is expected to enhance the performance and the dimensions of HPOT large receivers made up of several OPCs while minimizing semiconductor material usage [187–189].

Temperature. OPCs often operate outside their optimal temperature range, from cryogenic conditions (~-200 ºC) [190] to extreme heat scenarios (~180 ºC) [170], significantly impacting efficiency. Fundamentally, higher temperatures reduce the semiconductor E_g, limiting V_{OC}, and, ultimately, the η_{PV}. Furthermore, this issue particularly affects MJ horizontal architectures, where the bandgap and absorption coefficient variations can induce current mismatches among the subcells. To minimize this effect, and almost eliminate it, both the OPC structure and the laser wavelength must be optimized for the intended temperature operating conditions [191]. In this sense, it has been shown that performance degradation can be limited to a maximum of approximately 15% even under an extreme temperature variation range (~100 ºC) [192,193]. Additionally, mechanisms such as luminescent coupling, where photons emitted from radiative recombination in current-overproducing subcells are re-absorbed by current-limiting subcells, help mitigate current mismatches [194,195]. Nevertheless, the reduction in V_{OC} is considered the largest contributor to the performance degradation, as in standard solar cells [193,196]. [192]Extreme thermal stress can also end up damaging the cell or its components [197].

Additional strategies to mitigate temperature effects include the use of thermal packaging or cooling mechanisms [198]. Another promising approach involves integrating thermoelectric generators to maintain the OPC operating at its optimal point while simultaneously increasing $\eta_{E\text{-}E}$ by harnessing the excess heat [199]. Thermal losses can be further reduced by using wider bandgap semiconductors and increasing irradiance [200,201]. This approach reduces the absolute value of the temperature coefficient (T_C), a common parameter in PV for assessing the influence of temperature on device performance. These phenomena have been extensively studied and experimentally validated in MJ concentrator solar cells under ultra-high light intensities [202,203]. Fig. 12 shows the T_C of V_{OC}, the parameter that mainly explain the temperature dependence of PV devices, as a function of E_g for various illumination intensities in order to illustrate both effects previously mentioned [204].

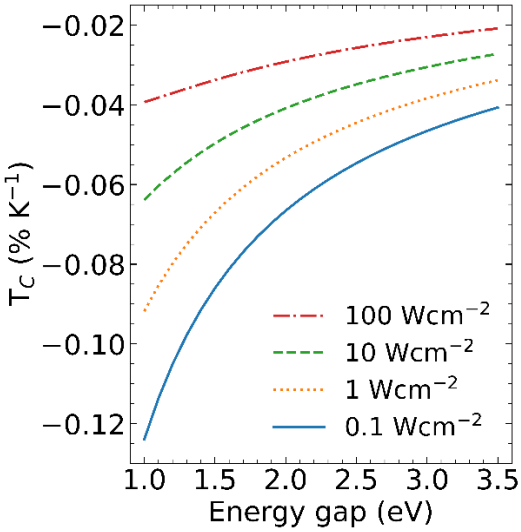

Fig. 12. Relative temperature coefficient (T_C) of open-circuit voltage (V_{OC}) at 298 K as a function of energy gap for various input light intensities. As a first approximation, it is considered that the temperature dependence of OPCs is primarily driven by variations in V_{OC}. The calculations are based on the radiative efficiency limit approach and using the expressions from Ref. [205], assuming negligible temperature-induced variations in the photo-generated current, fill factor and energy gap.

Nonetheless, OPCs often exhibit notable resilience to high-temperature conditions, maintaining a reduced but reliable level of functionality [170]

- *Other losses*: beyond the aforementioned sources, additional losses can further compromise OPC performance. These include optical losses, such as spillage losses, which occur when light falls outside the active area of the device [2,177], as well as misalignment losses, arising when light falls outside the acceptance angle of the cell [206]. Other common losses in conventional PV also apply, including thermal stress from sudden temperature variations (particularly under intermittent intense irradiance), mechanical strain, suboptimal system connections, humidity, soiling, and degradation due to radiation, to name a few [207,208].

Extrinsic losses have a critical negative impact on η_{PV}. Therefore, a thorough analysis and understanding of these losses are essential for advancing this technology.

5.3 OPCs performance overview

To illustrate the current capabilities of OPCs, Fig. 13 presents a comprehensive compilation of data reported in the literature that was accessible to the authors. The chart shows the maximum η_{PV} achieved by OPCs based on their semiconductor material as a function of the light source wavelength and ρ_{in}, represented using a red-tone scale. It should be noted that information regarding ρ_{in} is not always explicitly provided; in such cases, it was calculated from available data, assuming that the illuminated spot corresponded to the device active area unless specified otherwise. If the reference does not provide enough data to perform that estimation, the marker was left blank. Additionally, some results were obtained under broadband flash-lamp illuminations and converted to the desired wavelength using spectral response measurements, rather than directly using monochromatic sources. In light of the diversity of measurement approaches, standardization, although challenging [209–211], is urgently needed, not only to ensure reliability and quality of the results, but also to guarantee that measurements are reproducible and comparable across studies, as already emphasized by some researchers [183].

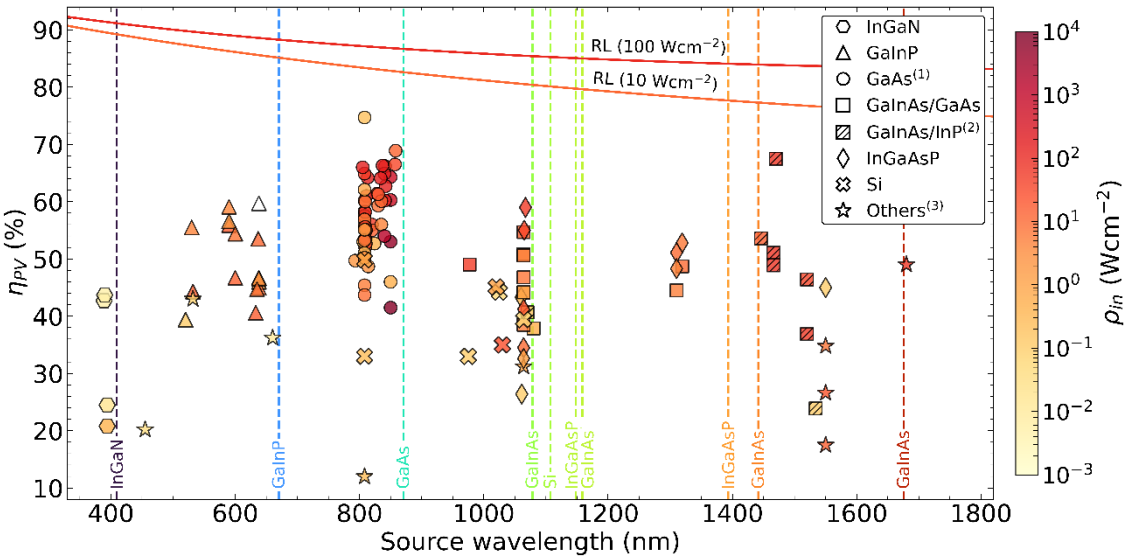

Fig. 13. Maximum photovoltaic efficiencies (η_{PV}) reported in literature as a function of light source wavelength [126,144,147,163,170,173,183,190,191,196,212–293]. Input power density (ρ_{in}) is represented with a logarithmic red-scale side-bar from 10^{-3} to 10^{4} Wcm^{-2} (marker left blank if required data is not provided). Relevant energy gaps for some of the most popular materials are represented as vertical dashed lines to easily visualized how close the laser wavelength is to this limit: InGaN (3.03 eV [294]), GaInP (1.85 eV [217]), GaAs (1.42 eV [283]), Si (1.12 eV [48]), GaInAs (1.15 eV [253], 1.07 eV [275], 0.86 eV [263], 0.74 eV [190,195]), InGaAsP (1.08 eV [291], 0.89 eV [263]). Grey curves represent the theoretical radiative efficiency limits (RL) at 10 and 100 Wcm^{-2} (assumptions described in Fig. 9, with R_S = 0). (1) Including AlGaAs and GaAs/AlGaAs heterostructures-based OPCs; (2) Including AlGaInAs-based OPCs; (3) Group consisting of CIS, CIGS, Ge, perovskites and organic OPCs.

As shown in Fig. 13, GaAs-based devices are by far the most abundant OPCs, accounting for roughly half of the total, and the most extensively studied, with early examples dating back to 1978 [42,295]. These devices achieve the highest η_{PV}, 34 of the top 35 efficiencies, including the room temperature (298 K) record of 68.9% at 858 nm [283], as well as the low temperature (150 K) record of 74.7% at 808 nm [196]. The success of GaAs can be attributed to its maturity, reliability, high efficiency, established presence across various PV fields, and the availability of lasers with suitable wavelengths [2,22,193]. Remarkably, the mean η_{PV} of over 50 GaAs-based OPCs gathered in this analysis is 56%.

In contrast, the efficiencies of other materials are significantly lower, generally under 55%, with the exception of a GaInAs-based OPC achieving a notable η_{PV} of 67.5% at 77 K, the third highest value [190]. For wavelengths greater than 900 nm, GaInAs and InGaAsP dominate, with η_{PV} up to 54.7% [253] and 52.8% [263], respectively, while GaSb is used for the longest wavelengths, exhibiting a 49.0% η_{PV} at 1680 nm [266]. For short wavelengths (<700 nm), GaInP leads with η_{PV} records of 59.7% at 638 nm [193], and 59.1% at 590 nm [289]. Recently, wide-bandgap OPCs based on InGaN demonstrated η_{PV} as high as 43.7% in the ultraviolet region (<400 nm), but at very low ρ_{in}, 5 mWcm^{-2} [214]. It is noteworthy that emerging PV technologies, such as thin-film CIS, CIGS, perovskites, and organic PV cells, are also gradually entering this field [222–226].

Most of the reported peak efficiencies are obtained within the 1 - 100 Wcm^{-2} range, except for extreme cases with tiny laser spots, of the order of hundredths of mm^2, notably elevating the power density to values well above 1000 W/cm^2 [235,259,270], or, conversely, other examples using very low-power lasers, operating at ρ_{in}~10^{-3} Wcm^{-2} [214,215].

For comparison with the ideal upper limit, the theoretical radiative efficiency limit for 10 and 100 Wcm^{-2} are also plotted in Fig. 13. The results indicate that OPCs based on the most developed

materials, such as GaAs and GaInAs, are impressively close to this limit, while materials with higher E_g, such as InGaN and GaInP, whose theoretical η_{PV} projections are even higher, still have significant room for improvement.

It is also important to mention that, while ρ_{in} serves as a useful metric for comparing device performance across studies, practical applications ultimately depend on their output power (P_{out}). To further contextualize the results, Fig. 14 presents data for the same OPCs shown in Fig. 13 in terms of their input and output power (P_{out}).

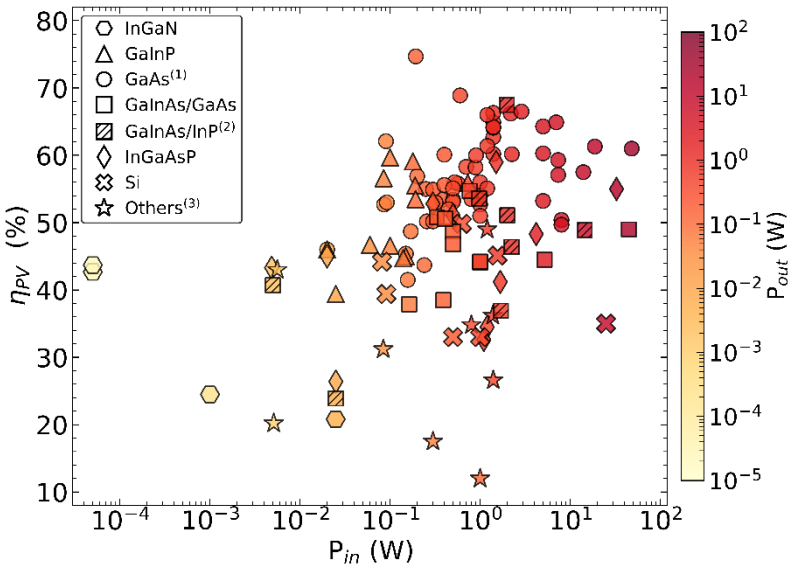

Fig. 14. Photovoltaic efficiency (η_{PV}) and output power (P_{out}) of the existing OPCs in literature versus their respective input power (P_{in}) [126,147,163,170,173,183,190,191,196,212–293]. In cases where data is not explicitly given, values are calculated from available information. (1) Including AlGaAs and GaAs/AlGaAs heterostructures-based OPCs; (2) Including AlGaInAs-based OPCs; (3) Group consisting of CIS, CIGS, Ge, perovskites and organic OPCs.

As expected, the most developed materials, GaAs and GaInAs, efficiently withstand P_{in} above 10 W, alongside a Si-based OPC achieving a remarkable 35.0% η_{PV} at P_{in}=25 W [126]. While fewer than 20% of the collected references report P_{out} exceeding 1 W, some OPCs are already capable of delivering over 20 W, with a maximum of 29.5 W at its peak η_{PV}, 61% [282], followed by 22 W at a η_{PV} of 49% [271]. Higher P_{out} values are certainly achievable, although this comes at the cost of a decrease in η_{PV}. This is strongly correlated with the size of the devices, as most OPCs are in the mm^2 range, where R_S and temperature losses begin to degrade performance at relatively low P_{in}. In practical terms, the implementation of OPCs would require further development of larger area devices while maintaining comparable performance levels, which may not be a trivial challenge.

Finally, it is worth mentioning that some OPCs are now commercially available from leading international suppliers such as Broadcom, Azur Space, or Spectrolab. This market availability represents a significant milestone in the maturation and commercialization of OPC technology, facilitating broader adoption and further development of these optoelectronic devices.

6. Applications and state-of-the-art HPOT systems

HPOT has recently gained widespread attention, entering an effervescent phase of practical development driven by its diverse applications and its potential to revolutionize the energy delivery paradigm. Highly versatile, this technology is adaptable to nearly any scenario. Unlike other WPT technologies based on capacitive, inductive, or magnetic resonance coupling, which are limited to near-field scenarios, HPOT stands out for its effective operation capability in far-

field applications, directly competing with microwave technology [28]. Nonetheless, it is important to emphasize that HPOT is certainly not adequate for every context; its suitability will depend on technical, economic, legal, and even social factors such as public acceptance. With this in mind, HPOT applications can be broadly divided into two main groups: space and terrestrial applications [1].

6.1 Space applications

Historically, power beaming has been closely tied to the space sector (see section 2 for more details). The absence of an atmosphere in space eliminates potential losses caused by suspended particles (mainly absorption, scattering, and thermal blooming), making HPOT ideal for in-space power transmission between satellites and spacecraft. This is particularly useful in scenarios with insufficient sunlight, such as eclipses, distant locations from the Sun, or powering small space vehicles with limited energy storage, or without light, such as the dark side of the Moon. Numerous studies have explored the fundamental challenges of satellite capabilities, focusing on crucial factors for the success of long-duration space missions, such as design, lifespan, and travel range [296–303].

The rapid progress in lunar exploration and industrialization is driving significant energy demands. Transmitting power to challenging regions, such as craters and permanently shadowed areas, remains a critical issue [1,304–306]. Given the faint atmosphere of the Moon (for most practical purposes it can be assumed vacuum [307]), optical energy transmission is expected to be efficient due to high η_T. As a result, various promising energy distribution strategies based on HPOT have been explored, including orbiting satellites and lunar power bases [22,24,38,40,41,308–314]. Similarly, HPOT systems have been proposed for other planets, such as Mars, whose rather thin atmosphere allows efficient optical energy propagation (with some absorption wavebands similar to Earth's [315]), and Venus, whose dense gaseous atmosphere limits transmission to a few viable windows [310,316].

Space application ambition does not stop there. Indeed, designs for space-based solar power (SBSP) stations and rocket propulsion supplying the energy from Earth to space utilizing large-scale HPOT systems have been studied [3,26,31,317–320]. Another remarkable benefit of HPOT technology is its potential ability to transfer uninterrupted, 24/7, clean solar energy harvested by future SBSP stations to Earth, thus mitigating the energy storage issues of terrestrial PV technology. This is, for instance, aligned with the ESA under the "SOLARIS - towards a clean and secure energy future for European citizens" initiative, which aims to cover 1/3 of the EU energy demand within the next decade [321]. This opens up novel frontiers to find unexplored resources to mitigate the energy and economic challenges of our era to contribute to the economic growth, improving the living conditions of humanity over the next decades [12].

6.2 Terrestrial applications

The variety of applications on Earth does not fall short of space applications. Demonstrating high precision tracking and robust safety features, HPOT technology is well-suited for both domestic and industrial environments [10]. It has been demonstrated that it is possible to wirelessly recharge via lasers small consumer electronic devices used in residential and workplace settings, such as smartphones, tablets, or cameras, enhancing user convenience [16]. HPOT also supports energy-demanding and mobile equipment commonly found in factory supply chains, like warehouse robots, boosting efficiency in high-volume manufacturing by enabling continuous operation [19,126].

In many cases, direct electrical power for electronic equipment is impractical or unsafe [2]. These restricted areas, generally called exclusion regions, include toxic environments and scenarios with high fire or explosion risks (e.g. refineries, mines, fuel tanks and aircrafts) [322,323], regions with intense electromagnetic interference (e.g. nuclear plants, high energy physics experiments) [324,325], and applications requiring galvanic insulation (e.g. high-voltage lines, lightning-

protected monitoring) [326–328]. Optical power transmission, either through air or fiber, minimizes these hazards. Moreover, HPOT enables simultaneous communication and power transmission [6,329,330], a key feature for sensors placed in harsh environments used in military missions [1,15] and for rechargeable batteries of medical devices, such as pacemakers and other body implants [17,18,331–333].

Other attractive terrestrial applications include not only remote powering of ground and aerial vehicles, such as rovers, unmanned aerial vehicles (UAVs), and small aircrafts [20–23,32,47,334], but also subaquatic equipment, like autonomous underwater vehicles (AUVs) [11,335–339]. By enabling energy replenishment at a distance, HPOT extends device mobility indefinitely, eliminating the need for interruptions to return to recharging stations. This allows for more efficient design, as less storage capacity is required, reducing weight. Such capabilities have a tremendous potential impact in numerous sectors, such as agriculture, security (e.g. rescue missions, disaster response), surveillance (e.g wildlife, environmental infrastructure, law enforcement, military), exploration missions (e.g deep ocean, extremely hot environments), communication (e.g. support to radio access networks), transportation, and entertainment [1,13]. In some of those fields, uninterrupted availability is imperative, and HPOT can meet these needs. Lastly, HPOT could enhance traditional power grids, offering a lightweight alternative to copper wires (fiber optic cables weigh 3.6 times less [32]).

6.3 Overview of HPOT experimental demonstrations

Optical power transmission is not a new concept, with experiments dating back to the late 20th century [226]. Since then, numerous proof-of-concept studies have been conducted, significantly increasing activity over the last decade. These experiments have targeted a wide range of applications, ranging from small aerial and underwater vehicles [20–23,296,309,334,336] to sensors and other electronic devices [32,228,340,341]. Recently, the first in-space HPOT was successfully demonstrated, proving the technology's capability to power real-world devices in various environments [298]. Fig. 15 presents an overview of reported HPOT experiments, showing their $\eta_{E\text{-}E}$, laser wavelengths employed, and transmission distances across different media: the atmosphere, water, fiber, and outer space.

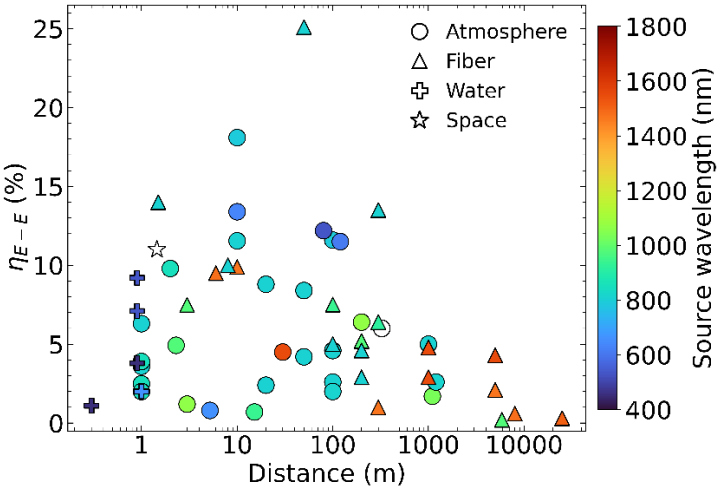

Fig. 15. Survey of the HPOT systems reported in the literature [6,12,20–23,32,33,126,207,227,228,239,277–280,296,298,299,309,330,334–338,340–361]. The figure shows the end-to-end efficiencies ($\eta_{E\text{-}E}$) and distances achieved by the gathered demonstrations. Data points are color-coded to indicate the light source wavelength and categorized by marker shape to represent the transmission medium: atmosphere, optical fiber, water, or outer space. White-colored markers indicate that the laser wavelength is not disclosed in the reference. Note: if $\eta_{E\text{-}E}$ is not explicitly provided, it is calculated as $\eta_{E\text{-}O} \times \eta_T \times \eta_{O\text{-}E}$. In cases where $\eta_{E\text{-}O}$ and/or $\eta_{O\text{-}}$

$_E$ are not detailed or cannot be estimated from available data, they are approximated as $\eta_{E\text{-}O}=\eta_S$ and $\eta_{O\text{-}E}=\eta_{PV}$. For more details on $\eta_{E\text{-}O}$, refer to the caption of Table 3.

The atmosphere is the most frequent medium for OWPT demonstrations, accounting for more than half of the documented experiments. These systems exhibit moderate $\eta_{E\text{-}E}$, generally below 10%, with transmission distances ranging from a few meters up to 1200 m, the longest reported distance for OWPT [309]. The highest $\eta_{E\text{-}E}$ achieved in atmospheric OWPT is 18.1% at a distance of 10 m [227]. GaAs-based OPCs are the most widely used, with lasers usually operating in the 800 - 900 nm waveband.

For underwater OWPT, the available examples are scarce. Due to the severe attenuation of water, transmission distances are limited to 1 meter or less, with $\eta_{E\text{-}E}$ usually lower than those of atmospheric OWPT, although a notable $\eta_{E\text{-}E}$ of 9.2% has been obtained (assuming a $\eta_{E\text{-}O}$ of 30%) [337]. The most efficient underwater systems rely on GaInP OPCs and employ 532 nm-wavelength lasers.

Regarding in-space OWPT, only one case has been reported to date, to the best of authors' knowledge. In 2023, approximately 1.5 W of almost uninterrupted power was transmitted for over 100 days to an OPC at a distance of 1.45 m, achieving a remarkable $\eta_{E\text{-}E}$ of around 11% [298]. Unfortunately, the material of the OPC and the light source wavelength were not disclosed.

Beyond OWPT systems, PoF systems have also been widely studied, with numerous reported experiments. Optical fibers enable transmissions over significantly longer distances than OWPT, reaching tens of kilometers [341,344,349,350]. Their efficiencies are similar to that of atmospheric OWPT systems, except for the record $\eta_{E\text{-}E}$ of 25.1%, achieved at a distance of 50 m [32]. 55% of the OPCs used in these systems are based on GaAs and GaInAs, with laser wavelengths around 800 - 900 nm and 1500 nm.

As for the emitter systems employed, Table 3 summarizes the available information about the light sources utilized in the experiments, all based in lasers. SCLs, particularly LDs, are the most widely used light source in the field due to their efficiency, versatility, and availability. Their broad spectral coverage across nearly the entire solar spectrum enables precise wavelength selection to optimize OPC performance, and they are capable of delivering relatively high P_S, enough for the targeted applications. For wavelengths longer than 1000 nm, fiber and SSLs are often used employed.

Table 3. Emitter systems used in HPOT experiments. The table provides information on the transmission medium, laser type, number of lasers employed, nominal power, wavelength, and electrical-to-optical efficiency ($\eta_{E\text{-}O}$). (*) indicates that $\eta_{E\text{-}O}$ is calculated from data included in the reference; if only η_S is provided, then $\eta_{E\text{-}O}=\eta_S$ is assumed. (**) When estimations defined in (*) cannot be performed due to insufficient information, $\eta_{E\text{-}O}$ = 30% is assumed. Note: Ref. [360] cautioned a η_S of few percent, thus a $\eta_{E\text{-}O}$ = 10% was assumed.

Medium	Type of laser	P_S (W)	λ (nm)	$\eta_{E\text{-}O}$ (%)	Reference
Atmosphere	LD	1500	940	50	[20]
	LD	1162	808	49	[278]
	LD	24	793	30	[239]
	LD	2500	810	**	[334]
	LD	500	808	47*	[22]
	LD	1.04	810	29*	[355]
	2x LD	-	660	27	[356]
	2x LD	200	808	30	[23]
	2x LD	2046	810	**	[361]
	3x LD	1.04	810	29*	[352]
	4x LD	1.53	850	30	[354]

	9x LD	1.53	850	**	[353]
	VCSEL	-	850	26*	[330]
	VCSEL	-	975	17	[351]
	5x VCSEL	2	850	42	[279]
	SCL	-	808	**	[207]
	SCL	-	808	**	[296]
	SCL	32	812	29*	[342]
	SCL	60	812	29*	[309]
	Disk	8000	1030	34	[126]
	Fiber	800	1070	30	[359]
	Fiber	50	1550	13	[280]
	Fiber	1.2	635	**	[277]
	SSL	8	532	**	[21]
	SSL	200	1064	**	[360]
	SSL	-	609	**	[357]
Fiber	LD	-	1550	15	[350]
	LD	1	810	**	[228]
	LD	0.25	1550	12*	[350]
	LD	15	1470	15	[350]
	LD	15	809	31*	[6]
	LD	12	808	37*	[299]
	LD	10	976	36*	[33]
	LD	2	1470	14*	[344]
	LD	15	808	45	[32]
	LD	0.5	1510	11*	[349]
	LD	30	915	30	[343]
	LD	30	940	30	[343]
	3x LD	1	976	**	[340]
	4x LD	35	808	45	[348]
	5x LD	3	808	15	[345]
	4x SCL	1.5	808	16	[346]
	Fiber	10	1480	8	[341]
	Fiber	3	1480	**	[347]
Water	LD	500	450	50	[336]
	LD	0.1	661	46	[335]
	Fiber	-	532	**	[337]

Finally, the adoption of international standards for reporting experimental results of HPOT is strongly encouraged, as many reviewed references lack meaningful information.

7. Conclusions

The emergence of high-power optical transmission (HPOT) technology entails a potential shift of the energy delivery paradigm as it is understood today. This transformative technology offers the prospect of reaching previously inaccessible locations, from the deep sea to outer space, enabling sustainable remote power transmission of kilowatts over distances of hundreds of kilometers. Optical power is immune to electromagnetic noise, provides galvanic insulation, and allows the simultaneous transfer of power and data. Consequently, HPOT presents a smart alternative to traditional wiring in scenarios where the latter is risky, or simply neither feasible nor

recommended. Although the concept originated decades ago, it is only now, driven by the need to meet emerging application demands where traditional technology is unfeasible, that HPOT is flourishing.

This works aims to provide a comprehensive review of HPOT systems, both optical wireless power transmission (OWPT) and power-over-fiber (PoF), examining their components, applications, and recent technological advancements. Following a brief historical overview of the origins and the evolution of HPOT, the emitter system is discussed, where different types of potential light sources are identified. Based on the requirements of HPOT, lasers emerge as a clear choice, although other prospective alternatives may play a role in the future. Among lasers, semiconductor ones, particularly laser diodes, stand out for their high efficiency, availability, and relatively low-cost. For long-distance, power-demanding applications, however, diode-pumped solid-state lasers may be a more appropriate choice mainly due to their high output powers.

The selection of the light source is heavily influenced by the medium through which transmission occurs. Attenuation of optical energy is a key concern, as a substantial fraction of the emitted power could be lost on their way to the target. Therefore, it is crucial to analyze the specific attenuation pattern of the medium to select optimal wavebands for transmission. In atmospheric and underwater applications, other phenomena, such as divergence, turbulence, and thermal blooming, also significantly affect light propagation and must be carefully considered and mitigated where possible. In turbulent media or using extreme high-power beams, system performance may be severely compromised. Additionally, beam divergence must be controlled to ensure practical implementation.

A thorough analysis of optical photovoltaic converters (OPCs) is also carried out, with special emphasis on their intrinsic and extrinsic loss mechanisms and corresponding mitigation strategies. Performance degradation due to series resistance, temperature, and beam non-uniformity are identified as major challenges that these devices must overcome to reach higher efficiency levels. Furthermore, a comprehensive compilation of OPCs results from the literature is presented, illustrating the clear dominance of GaAs and related semiconductors. Noteworthy efficiencies of 68.9% (298 K) and 74.7% (150 K) have been achieved at wavelengths of 858 and 808 nm, respectively. However, both shorter (<700 nm) and longer (>900 nm) wavelengths remain areas where, theoretically, OPCs have still room to improve, with ongoing research indicating progress in this regard.

Finally, the potential applications of HPOT systems for both terrestrial and space environments are explored. The range of possibilities is vast, including the powering of rovers, aerial and subaquatic vehicles, sensors, pacemakers, and satellites, to name a few cases. HPOT is set to make an immediate impact in sectors such as energy, defense, and healthcare, among others, significantly enhancing their capabilities. Moreover, the HPOT demonstrations conducted to date, to the best of the authors' knowledge, are presented, covering all types of transmission media: atmosphere, water, space, and fiber optics. Remarkable transmission distances exceeding 10 km and end-to-end efficiencies of 25.1% have already been achieved, reflecting persistent efforts to drive technological progress and boost overall performance.

This work provides an overview of HPOT technology, highlighting key milestones and offering perspective on the results reported in the literature. It presents the current state of the art, identifies both strengths and weaknesses, and suggests potential development pathways for improving system performance. While significant progress has been made, further work is necessary to enhance the efficiency of both emitter and receiver systems, as well as to mitigate light propagation losses, given the current limitations in overall performance. Nonetheless, considering the broad range of potential applications and recent technological advancements, HPOT holds the promise to revolutionize the energy sector, opening new horizons previously thought unattainable. Among this, it opens the possibility to transfer uninterrupted, 24/7, clean solar energy harvested by future space-based solar power stations to earth, thus mitigating the energy storage issues of terrestrial PV technology. This paves the way for discovering untapped resources

to address the energy and economic challenges of our time, fostering economic growth and enhancing living standards for humanity in the coming decades.

Acknowledgments

The work is part for the project PowerForEarth (PID2023-147898OB-I00) founded by MICIU/AEI /10.13039/501100011033/ and by ERDF, a way of making Europe. Also, the part of the work addressing space applications is part of the project RePowerSiC (Cod. 101160868), funded by European Union under the EIC Pathfinder Challenge (HORIZON-EIC-2023-PATHFINDERCHALLENGES-01): In-space solar energy harvesting for innovative space applications. The work of Pablo Sanmartín has been partially supported by the Subvenciones a la contratación y a la movilidad de personal investigador predoctoral en formación (PRE_2024_00803), funded by Junta de Andalucía.

CRediT authorship contribution statement

Pablo Sanmartín: Writing – original draft, Visualization, Validation, Software, Methodology, Investigation, Formal analysis, Conceptualization. **Eduardo F. Fernández**: Writing – review & editing, Supervision, Methodology, Investigation, Conceptualization, Project administration, Funding acquisition. **Antonio García-Loureiro:** Writing – review & editing, Investigation, Project administration, Funding acquisition. **Florencia Almonacid**: Writing – review & editing, Investigation, Project administration, Funding acquisition.

Data availability

The data that has been used are open to stakeholders among request.

Declaration of competing interest

The authors declare that they have no known competing financial interests or personal relationships that could have appeared to influence the work reported in this paper.

References

[1] Jaffe P, Nugent T, Strassner II B, Szazynski M. Power Beaming. vol. 05. WORLD SCIENTIFIC; 2024. https://doi.org/10.1142/12438.

[2] Algora C, García I, Delgado M, Peña R, Vázquez C, Hinojosa M, et al. Beaming power: Photovoltaic laser power converters for power-by-light. Joule 2022;6:340–68. https://doi.org/10.1016/j.joule.2021.11.014.

[3] Kang H, Kim H, Hong J, Zhang R, Lee M, Hong T. Harnessing sunlight beyond earth: Sustainable vision of space-based solar power systems in smart grid. Renewable and Sustainable Energy Reviews 2024;202:114644. https://doi.org/10.1016/j.rser.2024.114644.

[4] Jin K, Zhou W. Wireless Laser Power Transmission: A Review of Recent Progress. IEEE Trans Power Electron 2019;34:3842–59. https://doi.org/10.1109/TPEL.2018.2853156.

[5] Dickinson R, Grey J. Lasers For Wireless Power Transmission 1999. https://doi.org/hdl/2014/16855.

[6] Helmers H, Armbruster C, von Ravenstein M, Derix D, Schoner C. 6-W Optical Power Link With Integrated Optical Data Transmission. IEEE Trans Power Electron 2020;35:7904–9. https://doi.org/10.1109/TPEL.2020.2967475.

[7] Miyamoto T. Optical Wireless Power Transmission. Handbook of Radio and Optical Networks Convergence, Singapore: Springer Nature Singapore; 2024, p. 1093–120. https://doi.org/10.1007/978-981-97-2282-2_67.

[8] Putra EP, Theivindran R, Hasnul H, Lee HJ, Ker PJ, Jamaludin MZ, et al. Technology update on patent and development trend of power over fiber: a critical review and future prospects. J Photonics Energy 2023;13. https://doi.org/10.1117/1.JPE.13.011001.

[9] Kare JT, Nugent TJ, Bashford D, Erickson CC, Bashford TW. Light curtain safety system, 2024.

[10] Liu W, Chau KT, Tian X, Wang H, Hua Z. Smart wireless power transfer — opportunities and challenges. Renewable and Sustainable Energy Reviews 2023;180:113298. https://doi.org/10.1016/j.rser.2023.113298.

[11] Wang D, Zhang J, Cui S, Bie Z, Chen F, Zhu C. The state-of-the-arts of underwater wireless power transfer: A comprehensive review and new perspectives. Renewable and Sustainable Energy Reviews 2024;189:113910. https://doi.org/10.1016/j.rser.2023.113910.

[12] Zheng Y, Zhang G, Huan Z, Zhang Y, Yuan G, Li Q, et al. Wireless laser power transmission: Recent progress and future challenges. Space Solar Power and Wireless Transmission 2024;1:17–26. https://doi.org/10.1016/j.sspwt.2023.12.001.

[13] Vázquez C, Altuna R, López-Cardona JD. Power over fiber in radio access networks: 5G and beyond. Journal of Optical Communications and Networking 2024;16:D119. https://doi.org/10.1364/JOCN.522900.

[14] Chhawchharia S, Sahoo SK, Balamurugan M, Sukchai S, Yanine F. Investigation of wireless power transfer applications with a focus on renewable energy. Renewable and Sustainable Energy Reviews 2018;91:888–902. https://doi.org/10.1016/j.rser.2018.04.101.

[15] Arroyave MA, Behera B, Cavanna F, Feld A, Guo F, Heindel A, et al. Characterization and Novel Application of Power Over Fiber for Electronics in a Harsh Environment, 2024.

[16] Iyer V, Bayati E, Nandakumar R, Majumdar A, Gollakota S. Charging a Smartphone Across a Room Using Lasers. Proc ACM Interact Mob Wearable Ubiquitous Technol 2018;1:1–21. https://doi.org/10.1145/3161163.

[17] Algora C, Peña R. Recharging the Battery of Implantable Biomedical Devices by Light. Artif Organs 2009;33:855–60. https://doi.org/10.1111/j.1525-1594.2009.00803.x.

[18] Setiawan Putra AW, Tanizawa M, Maruyama T. Optical Wireless Power Transmission Using Si Photovoltaic Through Air, Water, and Skin. IEEE Photonics Technology Letters 2019;31:157–60. https://doi.org/10.1109/LPT.2018.2887081.

[19] Kawashima N, Takeda K, Matsuoka H, Fujii Y, Yamamoto M. Laser Energy Transmission for a Wireless Energy Supply to Robots. ISARC Proceedings, 2005. https://doi.org/10.22260/ISARC2005/0068.

[20] Blackwell T. Recent demonstrations of Laser power beaming at DFRC and MSFC. AIP Conf Proc, AIP; 2005, p. 73–85. https://doi.org/10.1063/1.1925133.

[21] Steinsiek F, Weber KH, Foth WP, Foth HJ, Schafer C. Wireless power transmission experiment using an airship as relay system and a moveable rover as ground target for later planetary exploration missions. 8th ESA Workshop on Advanced Space Technologies for Robotics and Automation, 2004, p. 1–10.

[22] Xu H, Du B, Shi D, Huang X, Hou X. Laser wireless power transfer system design for lunar rover. Space Solar Power and Wireless Transmission 2024. https://doi.org/10.1016/j.sspwt.2024.09.005.

[23] Kawashima N, Takeda K, Yabe K. Application of the laser energy transmission technology to drive a small airplane. Chin Opt Lett 2007;5:S109–S110.

[24] Grandidier J, Jaffe P, Roberts WT, Wright MW, Fraeman AA, Raymond CA, et al. Laser Power Beaming for Lunar Night and Permanently Shadowed Regions. Bulletin of the AAS 2021;53. https://doi.org/10.3847/25c2cfeb.13f46900.

[25] Landis GA. Space power by ground-based laser illumination. IEEE Aerospace and Electronic Systems Magazine 1991;6:3–7. https://doi.org/10.1109/62.103777.

[26] Johnson W, Dahlburg K, Bartolo B, Dorsey W, Gubser D, Jenkins P, et al. Space-based Solar Power: Possible Defense Applications and Opportunities for NRL Contributions 2009:105.

[27] Fortune Business Insights. Wireless Power Transmission Market Size, Share & Industry Analysis, By Technology (Inductive Coupling, Magnetic Resonance, Capacitive, RF, Infrared, and Others), By End-User (Near-field (Consumer Electronics, Automotive, Healthcare, Defense, and Others) and Far-field (Consumer Electronics, Automotive, Healthcare, Defense, and Others), and Regional Forecast, 2024-2032. 2024.

[28] Mohsan SAH, Qian H, Amjad H. A comprehensive review of optical wireless power transfer technology. Frontiers of Information Technology & Electronic Engineering 2023;24:767–800. https://doi.org/10.1631/FITEE.2100443.

[29] Reynolds WT. Architecture analysis of wireless power transmission for lunar outposts. Monterey, California: Naval Postgraduate School, 2015.

[30] Aviv D. Laser space communications. Artech; 2006.

[31] Alam KS, Kaif AMAD, Das SK, Abhi SH, Muyeen SM, Ali MdF, et al. Towards net zero: A technological review on the potential of space-based solar power and wireless power transmission. Heliyon 2024;10:e29996. https://doi.org/10.1016/j.heliyon.2024.e29996.

[32] Rosolem JB, Bassan FR, de Oliveira MP, dos Santos AB, Wollinger LM. Demonstration of an In-Flight Entertainment System Using Power-over-Fiber. Photonics 2024;11:627. https://doi.org/10.3390/photonics11070627.

[33] Prajzler V, Zikmund M. Power over fiber using a multimode optical power with a core diameter of 50 μm. Opt Quantum Electron 2024;56:1307. https://doi.org/10.1007/s11082-024-07231-8.

[34] Asimov I. Reason. 1st ed. Astounding Science Fiction; 1941.

[35] Glaser PE. Power from the Sun: Its Future. Science (1979) 1968;162:857–61. https://doi.org/10.1126/science.162.3856.857.

[36] Robinson Jr WJ. The feasibility of wireless power transmission for an orbiting astronomical station. 1968.

[37] Williams MD, Kwon JH, Walker GH, Humes DH. Diode laser satellite systems for beamed power transmission. 1990.

[38] Williams M, Young R, Schuster G, Choi S, Dagle J, Coomes E, et al. Power Transmission by Laser Beam From Lunar-Synchronous Satellite. 1998.

[39] Landis G, Stavnes M, Bozek J, Oleson S. Space transfer with ground-based laser/electric propulsion. 28th Joint Propulsion Conference and Exhibit, Reston, Virigina: American Institute of Aeronautics and Astronautics; 1992. https://doi.org/10.2514/6.1992-3213.

[40] Landis GA. Moonbase night power by laser illumination. J Propuls Power 1992;8:251–4. https://doi.org/10.2514/3.23469.

[41] Landis GA. Laser Power Beaming for Lunar Polar Exploration. AIAA Propulsion and Energy 2020 Forum, Reston, Virginia: American Institute of Aeronautics and Astronautics; 2020. https://doi.org/10.2514/6.2020-3538.

[42] DeLoach BC, Miller RC, Kaufman S. Sound Alerter Powered Over an Optical Fiber. Bell System Technical Journal 1978;57:3309–16. https://doi.org/10.1002/j.1538-7305.1978.tb02205.x.

[43] Scopus, https://www.scopus.com/ (accessed December 2, 2024). Query: “high power optical transmission” or “high power optical transfer” or “optical power beaming” or “optical wireless power transmission” or “optical wireless power transfer” or “power over fiber” or “optical photovoltaic converter” or “photovoltaic laser power converter” or “photovoltaic power converter” or “laser power converter” or “photonic power converter”

[44] Xu W, Wang X, Li W, Li S, Lu C. Research on test and evaluation method of laser wireless power transmission system. EURASIP J Adv Signal Process 2022;2022:20. https://doi.org/10.1186/s13634-022-00852-9.

[45] Titterton DH. Military laser technology and systems . Boston: Artech House; 2015.

[46] Kare JT. Modular Laser Launch Architecture: Analysis and Beam Module Design. 2004.

[47] Mason R. Feasibility of Laser Power Transmission to a High-Altitude Unmanned Aerial Vehicle. Santa Monica, CA: 2011.

[48] Raible DE. Free Space Optical Communications with High Intensity Laser Power Beaming 2011.

[49] Maini AK. Lasers and optoelectronics: fundamentals, devices and applications. John Wiley & Sons; 2013.

[50] QPC Lasers, https://www.qpclasers.com/ (accessed March 4, 2025).

[51] AeroDIODE, https://www.aerodiode.com/ (accessed March 4, 2025).

[52] LASERLINE, https://www.laserline.com/en-int/ (accessed March 4, 2025).

[53] Noda S, Yoshida M, Inoue T. The Brightest Semiconductor Laser Ever: Photonic Crystals Enable Tiny Lasers to Melt Steel. IEEE Spectr 2024;61:22–57. https://doi.org/10.1109/MSPEC.2024.10522928.

[54] Hill CH, Munro CW, Orchard JR, Javed I, Ivanov P, Gerrard ND, et al. Power Scaling of InP based Photonic Crystal Surface Emitting Lasers for CWDM Optical Interconnects in Hyperscale Datacenters. 2022 28th International Semiconductor Laser Conference (ISLC), IEEE; 2022, p. 1–2. https://doi.org/10.23919/ISLC52947.2022.9943354.

[55] King BC, Rae KJ, McKenzie AF, Boldin A, Kim D, Gerrard ND, et al. Coherent power scaling in photonic crystal surface emitting laser arrays. AIP Adv 2021;11. https://doi.org/10.1063/5.0031158.

[56] Taylor RJE, Childs DTD, Ivanov P, Stevens BJ, Babazadeh N, Sarma J, et al. Coherently Coupled Photonic-Crystal Surface-Emitting Laser Array. IEEE Journal of Selected Topics in Quantum Electronics 2015;21:493–9. https://doi.org/10.1109/JSTQE.2015.2417998.

[57] Ohnishi D, Okano T, Imada M, Noda S. Room temperature continuous wave operation of a surface-emitting two-dimensional photonic crystal diode laser. Opt Express 2004;12:1562. https://doi.org/10.1364/OPEX.12.001562.

[58] Kurosaka Y, Iwahashi S, Liang Y, Sakai K, Miyai E, Kunishi W, et al. On-chip beam-steering photonic-crystal lasers. Nat Photonics 2010;4:447–50. https://doi.org/10.1038/nphoton.2010.118.

[59] Kurosaka Y, Sakai K, Miyai E, Noda S. Controlling vertical optical confinement in two-dimensional surface-emitting photonic-crystal lasers by shape of air holes. Opt Express 2008;16:18485. https://doi.org/10.1364/OE.16.018485.

[60] Hirose K, Liang Y, Kurosaka Y, Watanabe A, Sugiyama T, Noda S. Watt-class high-power, high-beam-quality photonic-crystal lasers. Nat Photonics 2014;8:406–11. https://doi.org/10.1038/nphoton.2014.75.

[61] Noda S, Kitamura K, Okino T, Yasuda D, Tanaka Y. Photonic-Crystal Surface-Emitting Lasers: Review and Introduction of Modulated-Photonic Crystals. IEEE Journal of Selected Topics in Quantum Electronics 2017;23:1–7. https://doi.org/10.1109/JSTQE.2017.2696883.

[62] Noda S, Yokoyama M, Imada M, Chutinan A, Mochizuki M. Polarization Mode Control of Two-Dimensional Photonic Crystal Laser by Unit Cell Structure Design. Science (1979) 2001;293:1123–5. https://doi.org/10.1126/science.1061738.

[63] Yoshida M, Katsuno S, Inoue T, Gelleta J, Izumi K, De Zoysa M, et al. High-brightness scalable continuous-wave single-mode photonic-crystal laser. Nature 2023;618:727–32. https://doi.org/10.1038/s41586-023-06059-8.

[64] Scheps R. Introduction to Laser Diode-Pumped Solid State Lasers. SPIE; 2002. https://doi.org/10.1117/3.2279412.

[65] Franken PA, Hill AE, Peters CW, Weinreich G. Generation of Optical Harmonics. Phys Rev Lett 1961;7:118–9. https://doi.org/10.1103/PhysRevLett.7.118.

[66] Xue QH, Zheng Q, Bu YK, Jia FQ, Qian LS. High-power efficient diode-pumped Nd:YVO_4/LiB_3O_5457 nm blue laser with 46 W of output power. Opt Lett 2006;31:1070. https://doi.org/10.1364/OL.31.001070.

[67] Stolzenburg C, Schüle W, Zawischa I, Killi A, Sutter D. 700W intracavity-frequency doubled Yb:YAG thin-disk laser at 100 kHz repetition rate. In: Clarkson WA, Hodgson N, Shori RK, editors., 2010, p. 75780A. https://doi.org/10.1117/12.840875.

[68] Kablukov SI, Dontsova EI, Akulov VA, Vlasov AA, Babin SA. Frequency doubling of Yb-doped fiber laser to 515 nm. Laser Phys 2010;20:360–4. https://doi.org/10.1134/S1054660X10040043.

[69] IPG Photonics, https://www.ipgphotonics.com/ (accessed June 5, 2024).

[70] Zervas MN, Codemard CA. High Power Fiber Lasers: A Review. IEEE Journal of Selected Topics in Quantum Electronics 2014;20:219–41. https://doi.org/10.1109/JSTQE.2014.2321279.

[71] TRUMPF, https://www.trumpf.com/en_INT/ (accessed June 5, 2024).

[72] Havrilla D, Brockmann R. Disk laser: A new generation of industrial laser. International Congress on Applications of Lasers & Electro-Optics, Laser Institute of America; 2009, p. 151–8. https://doi.org/10.2351/1.5061524.

[73] Giesen A, Speiser J. Fifteen Years of Work on Thin-Disk Lasers: Results and Scaling Laws. IEEE Journal of Selected Topics in Quantum Electronics 2007;13:598–609. https://doi.org/10.1109/JSTQE.2007.897180.

[74] Krupke WF. Diode pumped alkali lasers (DPALs)—A review (rev1). Prog Quantum Electron 2012;36:4–28. https://doi.org/10.1016/j.pquantelec.2011.09.001.

[75] Beach RJ, Krupke WF, Kanz VK, Payne SA, Dubinskii MA, Merkle LD. End-pumped continuous-wave alkali vapor lasers: experiment, model, and power scaling. Journal of the Optical Society of America B 2004;21:2151. https://doi.org/10.1364/JOSAB.21.002151.

[76] Zhdanov B V., Knize RJ. Diode pumped alkali lasers. In: Titterton DH, Richardson MA, editors., 2011, p. 818707. https://doi.org/10.1117/12.897533.

[77] Cai H, Wang Y, Han J, An G, Zhang W, Xue L, et al. Reviews of a Diode-Pumped Alkali Laser (DPAL): a potential high powered light source. In: Hou X, Wang Z, Wu L, Ma J, editors., 2015, p. 95211U. https://doi.org/10.1117/12.2183410.

[78] Krupke WF. Diode pumped alkali lasers (DPALs): an overview. In: Phipps CR, editor., 2008, p. 700521. https://doi.org/10.1117/12.782466.

[79] Liu S, Tan R, Xu W, Ning F, Li Z. Double-Cycle Alternating-Flow Diode Pumped Potassium Vapor Laser. Photonics 2024;11:391. https://doi.org/10.3390/photonics11050391.

[80] Ren Guoguang 任国光, Yi Weiwei 伊炜伟, Qi Yu 齐 予, Huang Jijin 黄吉金, Qu Changhong 屈长虹. U.S. Theater and Strategic UVA-Borne Laser Weapon. Laser & Optoelectronics Progress 2017;54:100002. https://doi.org/10.3788/LOP54.100002.

[81] Wisoff P. Diode Pumped Alkaline Laser System: A High Powered, Low SWaP Directed Energy Option for Ballistic Missile Defense High-Level Summary. Livermore, CA (United States): 2017. https://doi.org/10.2172/1357366.

[82] Page RH, Boley CD, Rubenchik AM, Beach RJ. Diode Pumped Alkali Vapor Lasers - A New Pathway to High Beam Quality at High Average Power. Solid State and Diode Laser Technology Review, Livermore, CA (United States): 2005.

[83] Krupke WF. DPAL: A new class of lasers for cw power beaming at ideal photovoltaic cell wavelengths. AIP Conf Proc, AIP; 2004, p. 367–77. https://doi.org/10.1063/1.1721015.

[84] McNaught SJ, Asman CP, Injeyan H, Jankevics A, Johnson AMF, Jones GC, et al. 100-kW Coherently Combined Nd:YAG MOPA Laser Array. Frontiers in Optics 2009/Laser Science XXV/Fall 2009 OSA Optics & Photonics Technical Digest, Washington, D.C.: OSA; 2009, p. FThD2. https://doi.org/10.1364/FIO.2009.FThD2.

[85] Bayer A, Köhler B, Noeske A, Küster M, Irwin D, Patterson S, et al. Scalable and modular diode laser architecture for fiber coupling that combines high-power, high-brightness, and low weight. Proc.SPIE, vol. 8965, 2014, p. 89650J. https://doi.org/10.1117/12.2038959.

[86] Crump P, Erbert G, Wenzel H, Frevert C, Schultz CM, Hasler K-H, et al. Efficient High-Power Laser Diodes. IEEE Journal of Selected Topics in Quantum Electronics 2013;19:1501211–1501211. https://doi.org/10.1109/JSTQE.2013.2239961.

[87] Krupke WF. Diode-pumped alkali laser 2003.

[88] Berwal S, Khatri N, Kim D. A review on design modalities of solar-pumped solid-state laser. Applied Surface Science Advances 2022;12:100348. https://doi.org/10.1016/j.apsadv.2022.100348.

[89] Küblböck M, Will J, Fattahi H. Solar lasers: Why not? APL Photonics 2024;9. https://doi.org/10.1063/5.0209355.

[90] Castelletto S, Boretti A. Luminescence solar concentrators: A technology update. Nano Energy 2023;109:108269. https://doi.org/10.1016/j.nanoen.2023.108269.

[91] Collados MV, Chemisana D, Atencia J. Holographic solar energy systems: The role of optical elements. Renewable and Sustainable Energy Reviews 2016;59:130–40. https://doi.org/10.1016/j.rser.2015.12.260.

[92] Smith FG, Accetta JS, Shumaker DL. The Infrared & Electro-Optical Systems Handbook. Atmospheric Propagation of Radiation, Volume 2., 1993.

[93] Sprangle P, Hafizi B, Ting A, Fischer R. High-power lasers for directed-energy applications. Appl Opt 2015;54:F201. https://doi.org/10.1364/AO.54.00F201.

[94] Baker KS, Smith RC. Optical properties of the clearest natural waters (200–800 nm). Applied Optics, Vol 20, Issue 2, Pp 177-184 1981;20:177–84. https://doi.org/10.1364/AO.20.000177.

[95] Querry MR, Hale GM. Optical Constants of Water in the 200-nm to 200-μm Wavelength Region. Applied Optics, Vol 12, Issue 3, Pp 555-563 1973;12:555–63. https://doi.org/10.1364/AO.12.000555.

[96] Fernández EF, García-Loureiro A, Seoane N, Almonacid F. Band-gap material selection for remote high-power laser transmission. Solar Energy Materials and Solar Cells 2022;235. https://doi.org/10.1016/j.solmat.2021.111483.

[97] Hecht J. Understanding Fiber Optics. 2015. https://doi.org/https://doi.org/10.1117/3.1445658.

[98] Sanmartín P, Almonacid F, Ceballos MA, García-Loureiro A, Fernández EF. Wide-bandgap III-V materials for high efficiency air and underwater optical photovoltaic power transmission. Solar Energy Materials and Solar Cells 2024;266. https://doi.org/10.1016/j.solmat.2023.112662.

[99] Iqbal M. An introduction to solar radiation. Academic Press; 1983.

[100] Baykal Y, Ata Y, Gökçe MC. Underwater turbulence, its effects on optical wireless communication and imaging: A review. Opt Laser Technol 2022;156:108624. https://doi.org/10.1016/j.optlastec.2022.108624.

[101] Milonni PW, Eberly JH. Laser Physics. Wiley; 2010. https://doi.org/10.1002/9780470409718.

[102] Sprangle P, Hafizi B. High-power, high-intensity laser propagation and interactions. Phys Plasmas 2014;21. https://doi.org/10.1063/1.4878356.

[103] Spencer MF. Wave-optics investigation of turbulence thermal blooming interaction: I. Using steady-state simulations. Optical Engineering 2020;59:1. https://doi.org/10.1117/1.OE.59.8.081804.

[104] Zhu X, Yu W, Liu G, Zhang C. The influence of steady-state thermal blooming effect on the quality of underwater laser power transmission. AIP Adv 2024;14. https://doi.org/10.1063/5.0180853.

[105] Ahn K, Lee S-H, Park I-K, Yang H-S. Numerical simulation of high-energy laser propagation through the atmosphere and phase correction based on adaptive optics. Journal of the Korean Physical Society 2021;79:918–29. https://doi.org/10.1007/s40042-021-00293-x.

[106] Smith DC. High-power laser propagation: Thermal blooming. Proceedings of the IEEE 1977;65:1679–714. https://doi.org/10.1109/PROC.1977.10809.

[107] Reich S, Schäffer S, Lueck M, Wickert M, Osterholz J. Continuous wave high-power laser propagation in water is affected by strong thermal lensing and

thermal blooming already at short distances. Sci Rep 2021;11:22619. https://doi.org/10.1038/s41598-021-02112-6.

[108] Qiu D, Tian B, Ting H, Zhong Z, Zhang B. Mitigation of thermal blooming by rotating laser beams in the atmosphere. Appl Opt 2021;60:8458. https://doi.org/10.1364/AO.438485.

[109] Spencer MF, Cusumano SJ, Schmidt JD, Fiorino ST. Impact of spatial resolution on thermal blooming phase compensation instability. In: Dayton DC, Rhoadarmer TA, Sanchez DJ, editors., 2010, p. 781609. https://doi.org/10.1117/12.859936.

[110] Gebhardt FG. High power laser propagation. Appl Opt 1976;15:1479. https://doi.org/10.1364/AO.15.001479.

[111] Tyson RK, Ulrich PB. Adaptive Optics. The Infrared & Electro-Optical Systems Handbook, Vol. 8: Emerging Systems and Technologies, SPIE; 1993. https://doi.org/10.1117/3.2543827.ch2.

[112] Breaux H, Evers W, Sepucha R, Whitney C. Algebraic model for cw thermal-blooming effects. Appl Opt 1979;18:2638. https://doi.org/10.1364/AO.18.002638.

[113] Gupta PK, Khare R. Laser Physics and Technology. vol. 160. New Delhi: Springer India; 2015. https://doi.org/10.1007/978-81-322-2000-8.

[114] Davis Jr, DD, Mettler SC, DiGiovanni DJ. Comparative evaluation of fiber fuse models. In: Bennett HE, Guenther AH, Kozlowski MR, Newnam BE, Soileau MJ, editors., 1997, p. 592–606. https://doi.org/10.1117/12.274220.

[115] Dianov EM, Bufetov IA, Frolov AA, Mashinsky VM, Plotnichenko VG, Churbanov MF, et al. Catastrophic destruction of fluoride and chalcogenide optical fibres. Electron Lett 2002;38:783–4. https://doi.org/10.1049/el:20020539.

[116] Rosolem JB. Power-Over-Fiber Applications for Telecommunications and for Electric Utilities. Optical Fiber and Wireless Communications, InTech; 2017. https://doi.org/10.5772/68088.

[117] Shen YR, Bloembergen N. Theory of Stimulated Brillouin and Raman Scattering. Physical Review 1965;137:A1787–805. https://doi.org/10.1103/PhysRev.137.A1787.

[118] Keiser G. Nonlinear Processes in Optical Fibers. Fiber Optic Communications, Singapore: Springer Singapore; 2021, p. 477–506. https://doi.org/10.1007/978-981-33-4665-9_12.

[119] Al-Zubaidi FMA, Lopez-Cardona JD, Sanchez Montero D, Vazquez C. Optically Powered Radio-Over-Fiber Systems in Support of 5G Cellular Networks and IoT. Journal of Lightwave Technology 2021;39:4262–9. https://doi.org/10.1109/JLT.2021.3074193.

[120] Souza LC de, Souto VDP, Sodré AC. Radio- and Power-Over-Fiber Integration for 6G Networks: Challenges and Future Prospects. IEEE Access 2025;13:5321–41. https://doi.org/10.1109/ACCESS.2024.3523413.

[121] US Navy 100119-N-0365D-001 Members of the Directed Energy and Electric Weapon Systems Program Office fire a laser through a beam director on a Kineto

Tracking Mount, controlled by a MK-15 Phalanx Close-In Weapons System.jpg - Wikimedia Commons, https://commons.wikimedia.org/wiki/File:US_Navy_100119-N-0365D-001_Members_of_the_Directed_Energy_and_Electric_Weapon_Systems_Program_Office_fire_a_laser_through_a_beam_director_on_a_Kineto_Tracking_Mount,_controlled_by_a_MK-15_Phalanx_Close-In_Weapons_System.jpg (accessed July 25, 2024).

[122] Achtelik MC, Stumpf J, Gurdan D, Doth K-M. Design of a flexible high performance quadcopter platform breaking the MAV endurance record with laser power beaming. 2011 IEEE/RSJ International Conference on Intelligent Robots and Systems, IEEE; 2011, p. 5166–72. https://doi.org/10.1109/IROS.2011.6094731.

[123] Setiawan Putra AW, Kato H, Adinanta H, Maruyama T. Optical wireless power transmission to moving object using Galvano mirror. In: Hemmati H, Boroson DM, editors. Free-Space Laser Communications XXXII, SPIE; 2020, p. 50. https://doi.org/10.1117/12.2547424.

[124] Zhao M, Miyamoto T. LED Based Automatous Optical Wireless Power Transmission for Large Size Beam 2D Aiming. The 6th Optical Wireless and Fiber Power Transmission Conference (OWPT2024), Japan: 2024.

[125] Asaba K, Miyamoto T. Solar Cell Detection and Position, Attitude Determination by Differential Absorption Imaging in Optical Wireless Power Transmission. Photonics 2023;10:553. https://doi.org/10.3390/photonics10050553.

[126] Becker DE, Chiang R, Keys CC, Lyjak AW, Nees JA, Starch MD, et al. Photovoltaic-Concentrator Based Power Beaming For Space Elevator Application, 2010, p. 271–81. https://doi.org/10.1063/1.3435443.

[127] OSHA Technical Manual. U.S. Department of Labor, Occupational Safety and Health Administration, Office of Science and Technology Assessment; 1995.

[128] IEC 60825:2025 SER | IEC, https://webstore.iec.ch/en/publication/62424 (accessed February 12, 2025).

[129] ANSI Z136 Standards | The Laser Institute, https://www.lia.org/resources/laser-safety-information/laser-safety-standards/ansi-z136-standards (accessed July 25, 2024).

[130] ICNIRP Guidelines on Limits of Exposure to Laser Radiation of Wavelengths between 180 nm and 1,000 μm. Health Phys 2013;105:271–95. https://doi.org/10.1097/HP.0b013e3182983fd4.

[131] De Luca D, Delfino I, Lepore M. Laser Safety Standards and Measurements of Hazard Parameters for Medical Lasers. International Journal of Optics and Applications 2013;2:80–6. https://doi.org/10.5923/j.optics.20120206.01.

[132] Geeraets WJ, Berry ER. Ocular Spectral Characteristics as Related to Hazards from Lasers and Other Light Sources. Am J Ophthalmol 1968;66:15–20. https://doi.org/10.1016/0002-9394(68)91780-7.

[133] Nugent T, Summers J, Gort J, Weinthal W. Low-latency enhanced light curtain for safe laser power beaming. In: Jalali B, editor. Optical Power Delivery, SPIE; 2025, p. 5. https://doi.org/10.1117/12.3042366.

[134] Sliney DH. Radiation safety. The maximum permissible exposure levels: our knowledge of the hazards. Opt Laser Technol 1989;21:235–40. https://doi.org/10.1016/0030-3992(89)90082-0.

[135] Sweeney SJ, Eales TD, Jarvis SD, Mukherjee J. Optical wireless power at eye-safe wavelengths: Challenges and opportunities. Proceedings of the 3rd Optical Wireless and Fiber Power Transmission Conference (OWPT2021), Yokohama, Japan, 2021, p. 19–22.

[136] File:IEC60825 MPE W s.png - Wikimedia Commons, https://commons.wikimedia.org/wiki/File:IEC60825_MPE_W_s.png (accessed February 12, 2025).

[137] The Wireless Power Company | Wi-Charge, https://www.wi-charge.com/ (accessed July 30, 2024).

[138] Alpert O, Paschotta R. Wireless laser system for power transmission utilizing a gain medium between retroreflectors. 9312660, 2016.

[139] Fang W, Deng H, Liu Q, Liu M, Jiang Q, Yang L, et al. Safety Analysis of Long-Range and High-Power Wireless Power Transfer Using Resonant Beam. IEEE Transactions on Signal Processing 2021;69:2833–43. https://doi.org/10.1109/TSP.2021.3076893.

[140] Xiong M, Liu Q, Liu M, Wang X, Deng H. Resonant Beam Communications With Photovoltaic Receiver for Optical Data and Power Transfer. IEEE Transactions on Communications 2020;68:3033–41. https://doi.org/10.1109/TCOMM.2020.2973962.

[141] Summers J, Smith M, Gort J, Bashford T, Nugent T. Analysis and design of safe laser power beaming systems. In: Jalali B, editor. Optical Power Delivery, SPIE; 2025, p. 9. https://doi.org/10.1117/12.3043851.

[142] Aquila, https://www.aquila.earth/ (accessed July 30, 2024).

[143] Zuo C, Miyamoto T. Camera-Based Safety System for Optical Wireless Power Transmission Using Dynamic Safety-Distance. Photonics 2024;11:500. https://doi.org/10.3390/photonics11060500.

[144] Merz JL, Logan RA, McBride PL, Sergent AM. GaAs double-heterostructure photodetectors. J Appl Phys 1977;48:3580–7. https://doi.org/10.1063/1.324158.

[145] Lin M, Sha WEI, Zhong W, Xu D. Intrinsic losses in photovoltaic laser power converters. Appl Phys Lett 2021;118. https://doi.org/10.1063/5.0040144.

[146] Shockley W, Queisser HJ. Detailed Balance Limit of Efficiency of *p-n* Junction Solar Cells. J Appl Phys 1961;32:510–9. https://doi.org/10.1063/1.1736034.

[147] Bett AW, Dimroth F, Lockenhoff R, Oliva E, Schubert J. III–V solar cells under monochromatic illumination. 2008 33rd IEEE Photovoltaic Specialists Conference, IEEE; 2008, p. 1–5. https://doi.org/10.1109/PVSC.2008.4922910.

[148] Cotal H, Fetzer C, Boisvert J, Kinsey G, King R, Hebert P, et al. III–V multijunction solar cells for concentrating photovoltaics. Energy Environ Sci 2009;2:174–92. https://doi.org/10.1039/B809257E.

[149] Pérez-Higueras P, Ferrer-Rodríguez JP, Almonacid F, Fernández EF. Efficiency and acceptance angle of High Concentrator Photovoltaic modules: Current status and indoor measurements. Renewable and Sustainable Energy Reviews 2018;94:143–53. https://doi.org/10.1016/j.rser.2018.06.011.

[150] Rodrigo P, Fernández EF, Almonacid F, Pérez-Higueras PJ. Models for the electrical characterization of high concentration photovoltaic cells and modules: A review. Renewable and Sustainable Energy Reviews 2013;26:752–60. https://doi.org/10.1016/j.rser.2013.06.019.

[151] Green MA. Solar cells: Operating principles, technology, and system applications. 1982.

[152] Haug A. Auger recombination in direct-gap semiconductors: band-structure effects. Journal of Physics C: Solid State Physics 1983;16:4159–72. https://doi.org/10.1088/0022-3719/16/21/017.

[153] Vossier A, Hirsch B, Gordon JM. Is Auger recombination the ultimate performance limiter in concentrator solar cells? Appl Phys Lett 2010;97. https://doi.org/10.1063/1.3510474.

[154] Richter A, Glunz SW, Werner F, Schmidt J, Cuevas A. Improved quantitative description of Auger recombination in crystalline silicon. Phys Rev B 2012;86:165202. https://doi.org/10.1103/PhysRevB.86.165202.

[155] Ochoa M, Barrigón E, Barrutia L, García I, Rey-Stolle I, Algora C. Limiting factors on the semiconductor structure of III–V multijunction solar cells for ultra-high concentration (1000–5000 suns). Progress in Photovoltaics: Research and Applications 2016;24:1332–45. https://doi.org/10.1002/pip.2791.

[156] Espinet González P. Advances in the modeling, characterization and reliability of concentrator multijunction solar cells. Universidad Politécnica de Madrid, 2012. https://doi.org/10.20868/UPM.thesis.14620.

[157] Luo D, Su R, Zhang W, Gong Q, Zhu R. Minimizing non-radiative recombination losses in perovskite solar cells. Nat Rev Mater 2019;5:44–60. https://doi.org/10.1038/s41578-019-0151-y.

[158] Dhankhar M, Pal Singh O, Singh VN. Physical principles of losses in thin film solar cells and efficiency enhancement methods. Renewable and Sustainable Energy Reviews 2014;40:214–23. https://doi.org/10.1016/j.rser.2014.07.163.

[159] Soley SS, Verma S, Khatri N, Pokhriyal S. Advancing efficiency: comprehensive strategies for minimizing optical and electrical losses in group III-V compound tandem solar cells for future photovoltaic technology. Engineering Research Express 2024;6:032301. https://doi.org/10.1088/2631-8695/ad5c2d.

[160] Li M, Li Z, Wang M, Tang Z, Ma Z. Suppressing Shunt and Trap-Assisted Recombination in Organic Photovoltaic Devices For Improved Indoor Light Harvesting Efficiency. ACS Appl Energy Mater 2024;7:11900–9. https://doi.org/10.1021/acsaem.4c02271.

[161] Algora C, Diaz V. Design and optimization of very high power density monochromatic GaAs photovoltaic cells. IEEE Trans Electron Devices 1998;45:2047–54. https://doi.org/10.1109/16.711373.

[162] Algora C, Díaz V. Influence of Series Resistance on Guidelines for Manufacture of Concentrator p-on-n GaAs Solar Cells. Progress in Photovoltaics: Research and Applications 2000;8:211–25. https://doi.org/10.1002/(SICI)1099-159X(200003/04)8:2.

[163] Oliva E, Dimroth F, Bett AW. GaAs converters for high power densities of laser illumination. Progress in Photovoltaics: Research and Applications 2008;16:289–95. https://doi.org/10.1002/pip.811.

[164] Fernandez EF, Seoane N, Almonacid F, Garcia-Loureiro AJ. Vertical-tunnel-junction (VTJ) solar cell for ultra-high light concentrations (>2000 suns). IEEE Electron Device Letters 2018:1–1. https://doi.org/10.1109/LED.2018.2880240.

[165] Seoane N, Fernández EF, Almonacid F, García-Loureiro A. Ultra-efficient intrinsic-vertical-tunnel-junction structures for next-generation concentrator solar cells. Progress in Photovoltaics: Research and Applications 2021;29:231–7. https://doi.org/10.1002/pip.3369.

[166] Outes C, Fernandez EF, Seoane N, Almonacid F, Garcia-Loureiro AJ. GaAs Vertical-Tunnel-Junction Converter for Ultra-High Laser Power Transfer. IEEE Electron Device Letters 2021;42:1882–5. https://doi.org/10.1109/LED.2021.3121501.

[167] Lozano JF, Seoane N, Comesaña E, Almonacid F, Fernández EF, García-Loureiro A. Laser Power Converter Architectures Based on 3C-SiC with Efficiencies >80%. Solar RRL 2022;6. https://doi.org/10.1002/solr.202101077.

[168] Sater BL, Sater ND. High voltage silicon VMJ solar cells for up to 1000 suns intensities. Conference Record of the Twenty-Ninth IEEE Photovoltaic Specialists Conference, 2002., IEEE; 2002, p. 1019–22. https://doi.org/10.1109/PVSC.2002.1190778.

[169] Chemisana D, Teixidó O, Vaillon R. Silicon Vertical Multijunction Cell for Thermophotovoltaic Conversion. ACS Energy Lett 2023;8:3520–5. https://doi.org/10.1021/acsenergylett.3c01168.

[170] Gou Y, Mou Z, Wang H, Chen Y, Wang J, Yang H, et al. High-performance laser power converters with resistance to thermal annealing. Opt Express 2024;32:8335. https://doi.org/10.1364/OE.515130.

[171] Fernández-Domínguez E, Torres-Delgado G, Castanedo-Pérez R, Márquez-Marín J, Zelaya-Ángel O. Effects of rapid thermal annealing as back contacts activation treatment on CdS/CdTe multi-contacted solar cells. Superlattices Microstruct 2021;151:106832. https://doi.org/10.1016/j.spmi.2021.106832.

[172] Delgado M, García I, Hinojosa M, Algora C. Design and characterization of multijunction photovoltaic laser power converters for nonuniform irradiance light profiles. Progress in Photovoltaics: Research and Applications 2023;31:617–26. https://doi.org/10.1002/pip.3664.

[173] Rybalchenko D V., Mintairov SA, Salii RA, Shvarts MZ, Timoshina NKh, Kalyuzhnyy NA. Optimization of structural and growth parameters of metamorphic InGaAs photovoltaic converters grown by MOCVD. Semiconductors 2017;51:93–9. https://doi.org/10.1134/S1063782617010201.

[174] Cuevas A, López-Romero S. The combined effect of non-uniform illumination and series resistance on the open-circuit voltage of solar cells. Solar Cells 1984;11:163–73. https://doi.org/10.1016/0379-6787(84)90024-3.

[175] Valdivia CE, Wilkins MM, Chahal SS, Proulx F, Provost P-O, Masson DP, et al. Many-junction photovoltaic device performance under non-uniform high-concentration illumination, 2017, p. 070005. https://doi.org/10.1063/1.5001438.

[176] Yang Q, Yang H, Wang J, Gou Y, Li J, Zhou S. Research on the output characteristics of laser wireless power transmission system with nonuniform laser irradiation. Optical Engineering 2022;61. https://doi.org/10.1117/1.OE.61.6.067106.

[177] Peña R, Algora C. Evaluation of mismatch and non-uniform illumination losses in monolithically series-connected GaAs photovoltaic converters. Progress in Photovoltaics: Research and Applications 2003;11:139–50. https://doi.org/10.1002/pip.469.

[178] Wang A-C, Yin J-J, Yu S-Z, Sun Y-R. Multiple tunnel diode peaks in I–V curves of a multijunction laser power converter. Appl Phys Lett 2022;121. https://doi.org/10.1063/5.0109587.

[179] García I, Rey-Stolle I, Algora C. Performance analysis of AlGaAs/GaAs tunnel junctions for ultra-high concentration photovoltaics. J Phys D Appl Phys 2012;45:045101. https://doi.org/10.1088/0022-3727/45/4/045101.

[180] Beattie MN, Valdivia CE, Wilkins MM, Zamiri M, Kaller KLC, Tam MC, et al. High current density tunnel diodes for multi-junction photovoltaic devices on InP substrates. Appl Phys Lett 2021;118. https://doi.org/10.1063/5.0036053.

[181] Soresi S, Hamon G, Larrue A, Alvarez J, Pires MP, Decobert J. InP:S/AlInAs:C Tunnel Junction Grown by MOVPE for Photovoltaic Applications. Physica Status Solidi (a) 2018;215. https://doi.org/10.1002/pssa.201700427.

[182] Gou Y, Zhu L, Mou Z, Chen Y, Cheng Y, Wang J, et al. InP-based tunnel junctions for ultra-high concentration photovoltaics. Opt Express 2024;32:408. https://doi.org/10.1364/OE.510281.

[183] García I, Hinojosa M, Delgado M, Algora C. Photovoltaic laser power converters producing 21 W/cm2 at a conversion efficiency of 66.5%. Cell Rep Phys Sci 2024:102263. https://doi.org/10.1016/j.xcrp.2024.102263.

[184] Ortabasi U. PowerSphere: A Novel Photovoltaic Cavity Converter Using Low Bandgap TPV Cells for Efficient Conversion of High Power Laser Beams to Electricity. AIP Conf Proc, AIP; 2004, p. 142–52. https://doi.org/10.1063/1.1841889.

[185] He T, Pan G, Zheng G, Xu Z, Lv Z, Wu Q, et al. Experimentation and Analysis of Intra-Cavity Beam-Splitting Method to Enhance the Uniformity of Light in the Powersphere. Photonics 2024;11:128. https://doi.org/10.3390/photonics11020128.

[186] Ferrer-Rodríguez JP, Baig H, Fernández EF, Almonacid F, Mallick T, Pérez-Higueras P. Optical modeling of four Fresnel-based high-CPV units. Solar Energy 2017;155:805–15. https://doi.org/10.1016/j.solener.2017.07.027.

[187] Ferrer-Rodríguez JP, Fernández EF, Baig H, Almonacid F, Mallick T, Pérez-Higueras P. Development, indoor characterisation and comparison to optical modelling of four Fresnel-based high-CPV units equipped with refractive secondary optics. Solar Energy Materials and Solar Cells 2018;186:273–83. https://doi.org/10.1016/j.solmat.2018.06.050.

[188] Saura JM, Rodrigo PM, Almonacid FM, Chemisana D, Fernández EF. Experimental characterisation of irradiance and spectral non-uniformity and its impact on multi-junction solar cells: Refractive vs. reflective optics. Solar Energy Materials and Solar Cells 2021;225:111061. https://doi.org/10.1016/j.solmat.2021.111061.

[189] Saura JM, Chemisana D, Rodrigo PM, Almonacid FM, Fernández EF. Effect of non-uniformity on concentrator multi-junction solar cells equipped with refractive secondary optics under shading conditions. Energy 2022;238:122044. https://doi.org/10.1016/j.energy.2021.122044.

[190] Fafard S, Masson D. 67.5% Efficient InP-Based Laser Power Converters at 1470 nm at 77 K. Photonics 2024;11:130. https://doi.org/10.3390/photonics11020130.

[191] Höhn O, Walker AW, Bett AW, Helmers H. Optimal laser wavelength for efficient laser power converter operation over temperature. Appl Phys Lett 2016;108. https://doi.org/10.1063/1.4954014.

[192] Reichmuth SK, Helmers H, Philipps SP, Schachtner M, Siefer G, Bett AW. On the temperature dependence of dual-junction laser power converters. Progress in Photovoltaics: Research and Applications 2017;25:67–75. https://doi.org/10.1002/pip.2814.

[193] Fafard S, Masson DP. Perspective on photovoltaic optical power converters. J Appl Phys 2021;130. https://doi.org/10.1063/5.0070860.

[194] Lopez E, Höhn O, Schauerte M, Lackner D, Schachtner M, Reichmuth SK, et al. Experimental coupling process efficiency and benefits of back surface reflectors in photovoltaic multi-junction photonic power converters. Progress in Photovoltaics: Research and Applications 2021;29:461–70. https://doi.org/10.1002/pip.3391.

[195] Wang A-C, Sun Y-R, Yu S-Z, Yin J-J, Zhang W, Wang J, et al. A method to analyze current mismatch in a multijunction laser power converter based on I–V measurements. Appl Phys Lett 2021;118. https://doi.org/10.1063/5.0048466.

[196] Fafard S, Masson DP. 74.7% Efficient GaAs-Based Laser Power Converters at 808 nm at 150 K. Photonics 2022;9:579. https://doi.org/10.3390/photonics9080579.

[197] Vaillon R, Parola S, Lamnatou C, Chemisana D. Solar Cells Operating under Thermal Stress. Cell Rep Phys Sci 2020;1:100267. https://doi.org/10.1016/j.xcrp.2020.100267.

[198] Meng X, Li X, Kong D, Mallick TK, Liu C. Enhanced heat transfer characteristics using dimples in the receiving end of laser wireless power transmission system. Appl Therm Eng 2024;252:123619. https://doi.org/10.1016/j.applthermaleng.2024.123619.

[199] Valera-Albacete Á, Almonacid F, Rodrigo PM, Fernández EF. The Potential of a Hybrid Optical Photovoltaic Converter–Thermoelectric Receiver to Enhance Conversion Efficiency. IEEE Electron Device Letters 2023;44:1360–3. https://doi.org/10.1109/LED.2023.3288173.

[200] Dupré O, Vaillon R, Green MA. Physics of the temperature coefficients of solar cells. Solar Energy Materials and Solar Cells 2015;140:92–100. https://doi.org/10.1016/j.solmat.2015.03.025.

[201] Outes C, Fernández EF, Seoane N, Almonacid F, García-Loureiro AJ. Dependence of the vertical-tunnel-junction GaAs solar cell on concentration and temperature. IET Renewable Power Generation 2022;16:1577–88. https://doi.org/10.1049/rpg2.12456.

[202] Braun A, Katz EA, Gordon JM. Basic aspects of the temperature coefficients of concentrator solar cell performance parameters. Progress in Photovoltaics: Research and Applications 2013;21:1087–94. https://doi.org/10.1002/pip.2210.

[203] Braun A, Hirsch B, Vossier A, Katz EA, Gordon JM. Temperature dynamics of multijunction concentrator solar cells up to ultra-high irradiance. Progress in Photovoltaics: Research and Applications 2013;21:202–8. https://doi.org/10.1002/pip.1179.

[204] Siefer G, Bett AW. Analysis of temperature coefficients for III–V multi-junction concentrator cells. Progress in Photovoltaics: Research and Applications 2014;22:515–24. https://doi.org/10.1002/pip.2285.

[205] Geisz JF, Friedman DJ, Steiner MA, France RM, Song T. *Operando* Temperature Measurements of Photovoltaic Laser Power Converter Devices Under Continuous High-Intensity Illumination. IEEE J Photovolt 2023;13:808–13. https://doi.org/10.1109/JPHOTOV.2023.3304360.

[206] Green MA. Limiting photovoltaic monochromatic light conversion efficiency. Progress in Photovoltaics: Research and Applications 2001;9:257–61. https://doi.org/10.1002/PIP.375.

[207] Mou Z, Zhao B, Zhu L, Wang J, Deng G, Yang H, et al. Optimal Photovoltaic Array Configuration under Non-Uniform Laser Beam Conditions for Laser Wireless Power Transmission. Photonics 2024;11:193. https://doi.org/10.3390/photonics11030193.

[208] Rahman T, Mansur A, Hossain Lipu M, Rahman Md, Ashique R, Houran M, et al. Investigation of Degradation of Solar Photovoltaics: A Review of Aging Factors, Impacts, and Future Directions toward Sustainable Energy Management. Energies (Basel) 2023;16:3706. https://doi.org/10.3390/en16093706.

[209] Schachtner M, Beattie MN, Reichmuth SK, Wekkeli A, Siefer G, Helmers H. Measuring the device-level EQE of multi-junction photonic power converters. Progress in Photovoltaics: Research and Applications 2024;32:827–36. https://doi.org/10.1002/pip.3833.

[210] Shi L, Sun C, Liu Y, Liu K, Zhang W, Wu Y, et al. A novel method of determining bias lights for spectral response measurement of GaAs multi-junction laser power converters and its applications. Solar Energy Materials and Solar Cells 2024;266:112661. https://doi.org/10.1016/j.solmat.2023.112661.

[211] Zhang Y, Guan C, Chu W, Zhou Y, Zhou R, Yao Y. Optimal I–V Curve Scan Time for a GaAs Laser Power Converter. Photonics 2023;10:762. https://doi.org/10.3390/photonics10070762.

[212] Gou Y, Wang H, Wang J, Zhang Y, Niu R, Chen X, et al. 1064 nm InGaAs metamorphic laser power converts with over 44% efficiency. Opt Express 2022;30:42178. https://doi.org/10.1364/OE.474693.

[213] Koga M, Shibui S, Takahashi R, Suzuki J, Aoyama R, Noguchi T, et al. InGaN photovoltaic cells for applications in laser power beaming. In: Morkoç H, Fujioka H, Schwarz UT, editors. Gallium Nitride Materials and Devices XIX, SPIE; 2024, p. 24. https://doi.org/10.1117/12.3001576.

[214] Fujisawa T, Hu N, Kojima T, Egawa T, Miyoshi M. Over 43%-power-efficiency GaInN-based photoelectric transducer on free-standing GaN substrate for optical wireless power transmission system. Semicond Sci Technol 2024;39:045010. https://doi.org/10.1088/1361-6641/ad2d62.

[215] Miyoshi M, Nakabayashi T, Yamamoto K, Dalapati P, Egawa T. Improved epilayer qualities and electrical characteristics for GaInN multiple-quantum-well photovoltaic cells and their operation under artificial sunlight and monochromatic light illuminations. AIP Adv 2021;11. https://doi.org/10.1063/5.0062346.

[216] Pan H, Wang J, Chen X, Chen Y, Mou Z, Yang H, et al. InGaAs/GaAs metamorphic buffer for laser power converter applications. Opt Express 2024;32:48105. https://doi.org/10.1364/OE.544606.

[217] Sanmartín P, Fernández EF, García-Loureiro A, Montes-Romero J, Cano A, Martín P, et al. Design and Characterization of a 53.5% Efficient Gallium Indium Phosphide-Based Optical Photovoltaic Converter under 637 nm Laser Irradiation at 10 W cm $^{-2}$. Solar RRL 2024;8. https://doi.org/10.1002/solr.202400278.

[218] Chen Y, Mou Z, Wang J, Zhu L, Gou Y, Sun Z. 808 nm Laser Power Converters for Simultaneous Wireless Information and Power Transfer. IEEE J Photovolt 2024;14:890–900. https://doi.org/10.1109/JPHOTOV.2024.3423764.

[219] Wang A-C, Sun Y-R, Yu S-Z, Yin J-J, Zhang W, Wang J-S, et al. Characteristics of 1520 nm InGaAs multijunction laser power converters. Appl Phys Lett 2021;119. https://doi.org/10.1063/5.0073806.

[220] Helmers H, Oliva E, Schachtner M, Mikolasch G, Ruiz-Preciado LA, Franke A, et al. Overcoming optical-electrical grid design trade-offs for cm ^{2} -sized high-power GaAs photonic power converters by plating technology. Progress in Photovoltaics: Research and Applications 2024;32:636–42. https://doi.org/10.1002/pip.3804.

[221] Valdivia CE, Wilkins MM, Bouzazi B, Jaouad A, Aimez V, Arès R, et al. Five-volt vertically-stacked, single-cell GaAs photonic power converter. In: Freundlich A, Guillemoles J-F, Sugiyama M, editors., 2015, p. 93580E. https://doi.org/10.1117/12.2079824.

[222] Ishikawa R, Kato T, Anzo R, Nagatake M, Nishimura T, Tsuboi N, et al. Widegap CH3NH3PbBr3 solar cells for optical wireless power transmission application. Appl Phys Lett 2020;117. https://doi.org/10.1063/5.0010009.

[223] Wang Y, Zheng Z, Wang J, Bi P, Chen Z, Ren J, et al. Organic laser power converter for efficient wireless micro power transfer. Nat Commun 2023;14:5511. https://doi.org/10.1038/s41467-023-41270-1.

[224] Guo X, Chen X, Li Q, Zhang G, Ding G, Li F, et al. High-Efficiency Wide-Bandgap Perovskite Solar Cells for Laser Energy Transfer Underwater. Energy Technology 2023;11. https://doi.org/10.1002/ente.202300083.

[225] Shibui S, Maeda T, Koga M, Chiba M, Fujii S, Komaki H, et al. Optical wireless power transmission using CIGS solar cells. In: Freundlich A, Hinzer K, Collin S, Sellers IR, editors. Physics, Simulation, and Photonic Engineering of Photovoltaic Devices XIII, SPIE; 2024, p. 29. https://doi.org/10.1117/12.3001607.

[226] Yugami H, Kanamori Y, Arashi H, Niino M, Moro A, Eguchi K, et al. Field experiment of laser energy transmission and laser to electric conversion. IECEC-97 Proceedings of the Thirty-Second Intersociety Energy Conversion Engineering Conference (Cat. No.97CH6203), vol. 1, IEEE; 1997, p. 625–30. https://doi.org/10.1109/IECEC.1997.659262.

[227] He Tao 何滔, Yang Suhui 杨苏辉, Zhang Haiyang 张海洋, Zhao Changming 赵长明, Xu Peng 徐鹏, Hao Jiayin 郝嘉胤, et al. Experiment of Space Laser Energy Transmission and Conversion with High Efficiency. Chinese Journal of Lasers 2013;40:0317001. https://doi.org/10.3788/CJL201340.0317001.

[228] Bottger G, Dreschmann M, Klamouris C, Hubner M, Roger M, Bett AW, et al. An Optically Powered Video Camera Link. IEEE Photonics Technology Letters 2008;20:39–41. https://doi.org/10.1109/LPT.2007.912695.

[229] Gou Y, Wang H, Wang J, Chen Y, Mou Z, Chen Y, et al. High-performance laser power converts for wireless information transmission applications. Opt Express 2023;31:34937. https://doi.org/10.1364/OE.499213.

[230] Hirota M, Iio S, Ohta Y, Niwa Y, Miyamoto T. Wireless power transmission between a NIR VCSEL array and silicon solar cells. 2015 20th Microoptics Conference (MOC), IEEE; 2015, p. 1–2. https://doi.org/10.1109/MOC.2015.7416493.

[231] Yin J, Sun Y, Wang A, Yu S, Wang J, Fu Q, et al. High-Voltage 1064 nm InGaAsP Multijunction Laser Power Converters. IEEE Electron Device Letters 2022;43:1291–4. https://doi.org/10.1109/LED.2022.3183833.

[232] Khvostikov VP, Sorokina S V., Khvostikova OA, Nakhimovich M V., Shvarts Z. Ge-Based Photovoltaic Laser-Power Converters. IEEE J Photovolt 2023;13:254–9. https://doi.org/10.1109/JPHOTOV.2023.3237280.

[233] Khvostikov VP, Sorokina S V., Soldatenkov FYu, Timoshina NKh. GaSb-based photovoltaic laser-power converter for the wavelength $\lambda \approx 1550$ nm. Semiconductors 2015;49:1079–82. https://doi.org/10.1134/S1063782615080114.

[234] Helmers H, Franke A, Lackner D, Hohn O, Predan F, Dimroth F. 51% Efficient Photonic Power Converters for O-Band Wavelengths around 1310 nm. 2020 47th IEEE Photovoltaic Specialists Conference (PVSC), IEEE; 2020, p. 2471–4. https://doi.org/10.1109/PVSC45281.2020.9300717.

[235] Panchak AN, Pokrovskiy P V., Malevskiy DA, Larionov VR, Shvarts MZ. High-Efficiency Conversion of High-Power-Density Laser Radiation. Technical Physics Letters 2019;45:24–6. https://doi.org/10.1134/S1063785019010310.

[236] Kalyuzhnyy NA, Emelyanov VM, Mintairov SA, Shvarts MZ. InGaAs metamorphic laser (λ=1064 nm) power converters with over 44% efficiency, 2018, p. 110002. https://doi.org/10.1063/1.5053550.

[237] Raible DE, Dinca D, Nayfeh TH. Optical frequency optimization of a high intensity laser power beaming system utilizing VMJ photovoltaic cells. 2011 International Conference on Space Optical Systems and Applications (ICSOS), IEEE; 2011, p. 232–8. https://doi.org/10.1109/ICSOS.2011.5783675.

[238] Khvostikov VP, Sorokina S V., Khvostikova OA, Potapovich NS, Malevskaya A V., Nakhimovich M V., et al. GaSb photovoltaic cells for laser power conversion, 2019, p. 050007. https://doi.org/10.1063/1.5124192.

[239] He T, Yang S-H, Zhang H-Y, Zhao C-M, Zhang Y-C, Xu P, et al. High-Power High-Efficiency Laser Power Transmission at 100 m Using Optimized Multi-Cell GaAs Converter. Chinese Physics Letters 2014;31:104203. https://doi.org/10.1088/0256-307X/31/10/104203.

[240] Ding Y, Li Q, Lu Y, Wang J. TO-packaged, multi-junction GaAs laser power converter with output electric power over 1W. 2017 Conference on Lasers and Electro-Optics Pacific Rim (CLEO-PR), IEEE; 2017, p. 1–3. https://doi.org/10.1109/CLEOPR.2017.8118975.

[241] Fafard S, York MCA, Proulx F, Wilkins M, Valdivia CE, Bajcsy M, et al. Ultra-efficient N-junction photovoltaic cells with V<inf>OC</inf> > 14V at high optical input powers. 2016 IEEE 43rd Photovoltaic Specialists Conference (PVSC), IEEE; 2016, p. 2374–8. https://doi.org/10.1109/PVSC.2016.7750065.

[242] Zhao Y, Liang P, Ren H, Han P. Enhanced efficiency in 808 nm GaAs laser power converters via gradient doping. AIP Adv 2019;9. https://doi.org/10.1063/1.5109133.

[243] Khvostikov VP, Sorokina S V., Potapovich NS, Khvostikova OA, Timoshina NKh, Shvarts MZ. Modification of Photovoltaic Laser-Power (λ = 808 nm) Converters Grown by LPE. Semiconductors 2018;52:366–70. https://doi.org/10.1134/S1063782618030120.

[244] Fave A, Kaminski A, Gavand M, Mayet L, Laugier A. GaAs converter for high power laser diode. Conference Record of the Twenty Fifth IEEE Photovoltaic Specialists Conference - 1996, IEEE; 1996, p. 101–4. https://doi.org/10.1109/PVSC.1996.563957.

[245] Fahrenbruch AL, Lopez-Otero L, Werthern JG, Ta-Chung Wu. GaAs- and InAlGaAs-based concentrator-type cells for conversion of power transmitted by optical fibers. Conference Record of the Twenty Fifth IEEE Photovoltaic Specialists Conference - 1996, IEEE; 1996, p. 117–20. https://doi.org/10.1109/PVSC.1996.563961.

[246] Krut D, Sudharsanan R, Isshiki T, King R, Karam NH. A 53% High Efficiency GaAs Vertically Integrated Multi-junction Laser Power Converter. 2007 65th

Annual Device Research Conference, IEEE; 2007, p. 123–4. https://doi.org/10.1109/DRC.2007.4373680.

[247] Olsen LC, Huber DA, Dunham G, Addis FW. High efficiency monochromatic GaAs solar cells. The Conference Record of the Twenty-Second IEEE Photovoltaic Specialists Conference - 1991, IEEE; 1991, p. 419–24. https://doi.org/10.1109/PVSC.1991.169250.

[248] Khvostikov VP, Kalyuzhnyy NA, Mintairov SA, Sorokina S V., Potapovich NS, Emelyanov VM, et al. Photovoltaic laser-power converter based on AlGaAs/GaAs heterostructures. Semiconductors 2016;50:1220–4. https://doi.org/10.1134/S1063782616090128.

[249] Huang J, Sun Y, Zhao Y, Yu S, Dong J, Xue J, et al. Four-junction AlGaAs/GaAs laser power converter. Journal of Semiconductors 2018;39:044003. https://doi.org/10.1088/1674-4926/39/4/044003.

[250] Sun Y, Dong J, He Y, Zhao Y, Yu S, Xue J, et al. A six-junction GaAs laser power converter with different sizes of active aperture. Optoelectron Lett 2017;13:21–4. https://doi.org/10.1007/s11801-016-6193-8.

[251] Law HD, Ng WW, Nakano K, Dapkus PD, Stone DR. High efficiency InGaAsP photovoltaic power converter. IEEE Electron Device Letters 1981;2:26–7. https://doi.org/10.1109/EDL.1981.25327.

[252] Kalyuzhnyy NA, Emelyanov VM, Evstropov V V., Mintairov SA, Mintairov MA, Nahimovich M V., et al. Optimization of photoelectric parameters of InGaAs metamorphic laser (λ=1064 nm) power converters with over 50% efficiency. Solar Energy Materials and Solar Cells 2020;217:110710. https://doi.org/10.1016/j.solmat.2020.110710.

[253] Pellegrino C, Helmers H, Ohlmann J, Höhn O, Lackner D. High-Efficiency 1064 nm Metamorphic Photonic Power Converters for Spacecraft Wireless Power Transfer. 2023 13th European Space Power Conference (ESPC), IEEE; 2023, p. 1–4. https://doi.org/10.1109/ESPC59009.2023.10298134.

[254] Kim Y, Shin H-B, Lee W-H, Jung SH, Kim CZ, Kim H, et al. 1080 nm InGaAs laser power converters grown by MOCVD using InAlGaAs metamorphic buffer layers. Solar Energy Materials and Solar Cells 2019;200:109984. https://doi.org/10.1016/j.solmat.2019.109984.

[255] Singh N, Kin Fai Ho C, Nelvin Leong Y, Lee KEK, Wang H. InAlGaAs/InP-Based Laser Photovoltaic Converter at ~ 1070 nm. IEEE Electron Device Letters 2016;37:1154–7. https://doi.org/10.1109/LED.2016.2591015.

[256] Khvostikov VP, Sorokina S V., Potapovich NS, Levin R V., Marichev AE, Timoshina NKh, et al. GaInAsP/InP-Based Laser Power Converters (λ = 1064 nm). Semiconductors 2018;52:1748–53. https://doi.org/10.1134/S1063782618130079.

[257] Green MA, Zhao J, Wang A, Wenham SR. 45% efficient silicon photovoltaic cell under monochromatic light. IEEE Electron Device Letters 1992;13:317–8. https://doi.org/10.1109/55.145070.

[258] Kimovec R, Helmers H, Bett AW, Topič M. Comprehensive electrical loss analysis of monolithic interconnected multi-segment laser power converters.

Progress in Photovoltaics: Research and Applications 2019;27:199–209. https://doi.org/10.1002/pip.3075.

[259] Khvostikov VP, Vlasov AS, Pokrovskiy P V., Khvostikova OA, Panchak AN, Marukhina EP, et al. Characterization of ultra high power laser beam PV converters, 2019, p. 080003. https://doi.org/10.1063/1.5124213.

[260] Jomen R, Tanaka F, Akiba T, Ikeda M, Kiryu K, Matsushita M, et al. Conversion efficiencies of single-junction III–V solar cells based on InGaP, GaAs, InGaAsP, and InGaAs for laser wireless power transmission. Jpn J Appl Phys 2018;57:08RD12. https://doi.org/10.7567/JJAP.57.08RD12.

[261] Jarvis SD, Mukherjee J, Perren M, Sweeney SJ. Development and characterisation of laser power converters for optical power transfer applications. IET Optoelectronics 2014;8:64–70. https://doi.org/10.1049/iet-opt.2013.0066.

[262] Guan C, Li L, Ji H-M, Luo S, Xu P, Gao Q, et al. Fabrication and Characterization of a High-Power Assembly With a 20-Junction Monolithically Stacked Laser Power Converter. IEEE J Photovolt 2018;8:1355–62. https://doi.org/10.1109/JPHOTOV.2018.2841195.

[263] Beattie MN, Helmers H, Forcade GP, Valdivia CE, Hohn O, Hinzer K. InP- and GaAs-Based Photonic Power Converters Under O-Band Laser Illumination: Performance Analysis and Comparison. IEEE J Photovolt 2023;13:113–21. https://doi.org/10.1109/JPHOTOV.2022.3218938.

[264] Peña R, Algora C, Antón I. GaAs multiple photovoltaic converters with an efficiency of 45% for monochromatic illumination. Proceedings of 3rd World Conference on Photovoltaic Energy Conversion, Osaka, Japan: 2003, p. 228–31.

[265] Khvostikov V, Kalyuzhnyy N, Mintairov S, Potapovich N, Shvarts M, Sorokina S, et al. AlGaAs/GaAs photovoltaic converters for high power narrowband radiation, 2014, p. 21–4. https://doi.org/10.1063/1.4897019.

[266] Andreev V, Khvostikov V, Kalinovsky V, Lantratov V, Grilikhes V. High current density GaAs and GaSb photovoltaic cells for laser power beaming. Proceedings of the 3rd World Conference on Photovoltaic Energy Conversion, Osaka, Japan: 2003, p. 761–3.

[267] Schubert J, Oliva E, Dimroth F, Guter W, Loeckenhoff R, Bett AW. High-Voltage GaAs Photovoltaic Laser Power Converters. IEEE Trans Electron Devices 2009;56:170–5. https://doi.org/10.1109/TED.2008.2010603.

[268] Howell JT, O'Neil MJ, Fork RL. Advanced Receiver/Converter Experiments for Laser Wireless Power Transmission. Proceedings of The 4th International Conference on Solar Power from Space (SPS04), together with the 5th International Conference on Wireless Power Transmission, Granada, Spain: 2004.

[269] Reichmuth SK, Helmers H, Garza C, Vahle D, de Boer M, Stevens L, et al. Transient I-V Measurement Set-Up for Photovoltaic Laser Power Converters under Monochromatic Irradiance. 32nd European Photovoltaic Solar Energy Conference and Exhibition, Munich, Germany: 2016. https://doi.org/10.4229/EUPVSEC20162016-1AO.1.2.

[270] Khvostikov VP, Panchak AN, Khvostikova OA, Pokrovskiy Pavel V. Side-Input GaAs Laser Power Converters With Gradient AlGaAs Waveguide. IEEE Electron Device Letters 2022;43:1717–9. https://doi.org/10.1109/LED.2022.3202987.

[271] Fafard S, Masson D, Werthen J-G, Liu J, Wu T-C, Hundsberger C, et al. Power and Spectral Range Characteristics for Optical Power Converters. Energies (Basel) 2021;14:4395. https://doi.org/10.3390/en14154395.

[272] Huang J, Sun Y, Zhao Y, Yu S, Li K, Dong J, et al. Characterizations of high-voltage vertically-stacked GaAs laser power converter. Journal of Semiconductors 2018;39:094006. https://doi.org/10.1088/1674-4926/39/9/094006.

[273] Zhao Y, Sun Y, He Y, Yu S, Dong J. Design and fabrication of six-volt vertically-stacked GaAs photovoltaic power converter. Sci Rep 2016;6:38044. https://doi.org/10.1038/srep38044.

[274] Fafard S, Proulx F, York MCA, Richard LS, Provost PO, Arès R, et al. High-photovoltage GaAs vertical epitaxial monolithic heterostructures with 20 thin p/n junctions and a conversion efficiency of 60%. Appl Phys Lett 2016;109. https://doi.org/10.1063/1.4964120.

[275] Kalyuzhnyy NA, Emelyanov VM, Evstropov V V., Mintairov SA, Mintairov MA, Nahimovich M V., et al. Thermal and resistive losses in InGaAs metamorphic laser (λ = 1064 nm) power converters with over 50% efficiency, 2019, p. 050006. https://doi.org/10.1063/1.5124191.

[276] Shan T, Qi X. Design and optimization of GaAs photovoltaic converter for laser power beaming. Infrared Phys Technol 2015;71:144–50. https://doi.org/10.1016/j.infrared.2015.03.010.

[277] Wong YL, Shibui S, Koga M, Hayashi S, Uchida S. Optical Wireless Power Transmission Using a GaInP Power Converter Cell under High-Power 635 nm Laser Irradiation of 53.5 W/cm2. Energies (Basel) 2022;15:3690. https://doi.org/10.3390/en15103690.

[278] Gou Y, Wang H, Wang J, Niu R, Chen X, Wang B, et al. High-performance laser power converts for direct-energy applications. Opt Express 2022;30:31509. https://doi.org/10.1364/OE.470740.

[279] Katsuta Y, Miyamoto T. Design, simulation and characterization of fly-eye lens system for optical wireless power transmission. Jpn J Appl Phys 2019;58:SJJE02. https://doi.org/10.7567/1347-4065/ab238b.

[280] Mukherjee J, Jarvis S, Perren M, Sweeney SJ. Efficiency limits of laser power converters for optical power transfer applications. J Phys D Appl Phys 2013;46:264006. https://doi.org/10.1088/0022-3727/46/26/264006.

[281] Fafard S, Masson DP. High-Efficiency and High-Power Multijunction InGaAs/InP Photovoltaic Laser Power Converters for 1470 nm. Photonics 2022;9:438. https://doi.org/10.3390/photonics9070438.

[282] Fafard S, Masson D. Vertical Multi-Junction Laser Power Converters with 61% Efficiency at 30 W Output Power and with Tolerance to Beam Non-Uniformity, Partial Illumination, and Beam Displacement. Photonics 2023, Vol 10, Page 940 2023;10:940. https://doi.org/10.3390/PHOTONICS10080940.

[283] Helmers H, Lopez E, Höhn O, Lackner D, Schön J, Schauerte M, et al. 68.9% Efficient GaAs-Based Photonic Power Conversion Enabled by Photon Recycling and Optical Resonance. Physica Status Solidi - Rapid Research Letters 2021;15. https://doi.org/10.1002/pssr.202100113.

[284] Kurooka K, Honda T, Komazawa Y, Warigaya R, Uchida S. A 46.7% efficient GaInP photonic power converter under high-power 638 nm laser uniform irradiation of 1.5 W cm-2. Applied Physics Express 2022;15. https://doi.org/10.35848/1882-0786/ac67bb.

[285] Komuro Y, Honda S, Kurooka K, Warigaya R, Tanaka F, Uchida S. A 43.0% efficient GaInP photonic power converter with a distributed Bragg reflector under high-power 638nm laser irradiation of 17Wcm-2. Applied Physics Express 2021;14. https://doi.org/10.35848/1882-0786/abf31c.

[286] Fafard S, York MCA, Proulx F, Valdivia CE, Wilkins MM, Arès R, et al. Ultrahigh efficiencies in vertical epitaxial heterostructure architectures. Appl Phys Lett 2016;108. https://doi.org/10.1063/1.4941240.

[287] Mintairov SA, Evstropov V V., Mintairov MA, Nakhimovich M V., Salii RA, Shvarts MZ, et al. A GaInP-Based Photo-Converter of Laser Radiation with an Efficiency of 46.7% at a Wavelength of 600 nm. Technical Physics Letters 2023;49:S78–80. https://doi.org/10.1134/S106378502390042X.

[288] Mintairov SA, Malevskaya A V., Mintairov MA, Nakhimovich M V., Salii RA, Shvarts MZ, et al. High-Efficiency GaInP/GaAs Photoconverters of the 600 nm Laser Line. Technical Physics Letters 2023;49:S75–7. https://doi.org/10.1134/S1063785023900418.

[289] Klitzke M, Höhn O, Siefer G, Helmers H, Dimroth F, Lackner D. Rear-heterojunction GaInP laser power converter with 59% monochromatic efficiency at 590 nm. APL Photonics 2025;10. https://doi.org/10.1063/5.0249453.

[290] Kim B, Kim M, Li BD, Hool RD, Lee ML. Cryogenic GaAs laser power converters. Solar Energy Materials and Solar Cells 2025;281:113321. https://doi.org/10.1016/j.solmat.2024.113321.

[291] Yin J, Sun Y, Yu S, Zhao Y, Li R, Dong J. 1064 nm InGaAsP multi-junction laser power converters. Journal of Semiconductors 2020;41:062303. https://doi.org/10.1088/1674-4926/41/6/062303.

[292] Fafard S, Masson D. 55% Efficient High-Power Multijunction Photovoltaic Laser Power Converters for 1070 nm. Photonics 2025;12:406. https://doi.org/10.3390/photonics12050406.

[293] Forcade GP, Wilson DP, Beattie MN, Pellegrino C, Helmers H, Hunter RFH, et al. Multi-junction laser power converters exceeding 50% efficiency in the short wavelength infrared. Cell Rep Phys Sci 2025;6:102610. https://doi.org/10.1016/j.xcrp.2025.102610.

[294] Wu J, Walukiewicz W. Band gaps of InN and group III nitride alloys. Superlattices Microstruct 2003;34:63–75. https://doi.org/10.1016/J.SPMI.2004.03.069.

[295] Ilegems M, Schwartz B, Koszi LA, Miller RC. Integrated multijunction GaAs photodetector with high output voltage. Appl Phys Lett 1978;33:629–31. https://doi.org/10.1063/1.90443.

[296] Shi D, Zhang L, Ma H, Wang Z, Wang Y, Cui Z. Research on Wireless Power transmission system between satellites. 2016 IEEE Wireless Power Transfer Conference, WPTC 2016 2016. https://doi.org/10.1109/WPT.2016.7498851.

[297] Sanders M, Kang JS. Utilization of Polychromatic Laser System for Satellite Power Beaming. IEEE Aerospace Conference Proceedings 2020. https://doi.org/10.1109/AERO47225.2020.9172561.

[298] U.S. Naval Research Laboratory. First In-Space Laser Power Beaming Experiment Surpasses 100 Days of Successful On-Orbit Operations, https://www.spoc.spaceforce.mil/News/Article-Display/Article/3457469/first-in-space-laser-power-beaming-experiment-surpasses-100-days-of-successful (accessed March 11, 2024).

[299] Peña R, Algora C. One-watt fiber-based power-by-light system for satellite applications. Progress in Photovoltaics: Research and Applications 2012;20:117–23. https://doi.org/10.1002/pip.1130.

[300] Landis GA. Satellite eclipse power by laser illumination. Acta Astronaut 1991;25:229–33. https://doi.org/10.1016/0094-5765(91)90075-G.

[301] Cougnet C, Sein E, Celeste A, Summerer L. Solar Power Satellites for Space Exploration and Applications. In: Lacoste H, Ouwehand L, editors. Solar Power from Space - SPS 2004, vol. 567, 2004, p. 151.

[302] Steinsiek F. Wireless Power Transmission Experiment as an Early Contribution to Planetary Exploration Missions. 54th International Astronautical Congress of the International Astronautical Federation, the International Academy of Astronautics, and the International Institute of Space Law, Reston, Virigina: American Institute of Aeronautics and Astronautics; 2003. https://doi.org/10.2514/6.IAC-03-R.3.06.

[303] Thakar B, McNabb JT, Robertson BE, Mavris D. Trade Studies for Evaluating Lunar Surface Power Architectures. AIAA SCITECH 2025 Forum, Reston, Virginia: American Institute of Aeronautics and Astronautics; 2025. https://doi.org/10.2514/6.2025-2192.

[304] Zuniga AF, Turner MF, Rasky D, Loucks M, Carrico J, Policastri L. Building an Economical and Sustainable Lunar Infrastructure to Enable Lunar Industrialization. AIAA SPACE and Astronautics Forum and Exposition, Reston, Virginia: American Institute of Aeronautics and Astronautics; 2017. https://doi.org/10.2514/6.2017-5148.

[305] Bosquillon C, Cujko L, Gautel G, Webber D, Conconi A, Pianorsi M, et al. Is the Lunar Economy Solely for the Space Industry? Opportunities for Nonspace Companies in Lunar Infrastructure Leveraging Technological Synergies. New Space 2024;12:174–87. https://doi.org/10.1089/space.2023.0057.

[306] Besha P. Economic Growth and National Competitiveness Impacts of the Artemis Program. 2022.

[307] N. A. S. A., O'Neill GK. Space Settlements: A Design Study. University Press of the Pacific; 2004.

[308] Takeda K, Tanaka M, Miura S, Hashimoto K, Kawashima N. Laser power transmission for the energy supply to the rover exploring ice on the bottom of the crater in the lunar polar region. In: Basu S, Riker JF, editors., 2002, p. 223–7. https://doi.org/10.1117/12.469770.

[309] Takeda K, Kawashima N. 1.2 km Laser Energy Transmission for the Lunar Rover Model to Explore the Ice on the Moon. SPACE TECHNOLOGY JAPAN, THE JAPAN SOCIETY FOR AERONAUTICAL AND SPACE SCIENCES 2004;3:45–8. https://doi.org/10.2322/stj.3.45.

[310] Baraskar A, Yoshimura Y, Nagasaki S, Hanada T. Space solar power satellite for the Moon and Mars mission. Journal of Space Safety Engineering 2022;9:96–105. https://doi.org/10.1016/j.jsse.2021.10.008.

[311] Kerslake TW, El-Genk MS. Lunar Surface-to-Surface Power Transfer. AIP Conf Proc, AIP; 2008, p. 466–73. https://doi.org/10.1063/1.2845004.

[312] Lopez F, Mauro A, Mauro S, Monteleone G, Sfasciamuro DE, Villa A. A Lunar-Orbiting Satellite Constellation for Wireless Energy Supply. Aerospace 2023;10:919. https://doi.org/10.3390/aerospace10110919.

[313] Marcinkowski A, Carrio L, Hilliard S, Edwards C, Elhawary A, Clem D, et al. Lunar Surface Power Architecture Concepts. 2023 IEEE Aerospace Conference, IEEE; 2023, p. 1–19. https://doi.org/10.1109/AERO55745.2023.10115621.

[314] Fujita K. Laser Power Transmission on the Moon Using Multibeams of Single-Mode Fiber Lasers as Wireless System and Optical Fibers as Wired System. Journal of Evolving Space Activities 2024;2. https://doi.org/10.57350/jesa.174.

[315] Annis J. The Atmosphere of Mars and Optical Communications. Pasaden,CA: 1987.

[316] Grandidier J, Akins A, Crisp D, Lee YJ, Schwartz J, Bugga R, et al. Feasibility of power beaming through the Venus atmosphere. Acta Astronaut 2023;211:376–81. https://doi.org/10.1016/j.actaastro.2023.06.042.

[317] Jaffe P, Browne C, Depuma C, Longbottom L, Nisar H, Simlot V, et al. Opportunities and Challenges for Space Solar for Remote Installations 2019.

[318] Resendes D, Mota S, Mendonca J, Sanders B, Encarnação J, Gonzalez del Amo J. Laser Propulsion for Ground to Orbit Launch. IEPC 2005.

[319] Kantrowitz A. Propulsion to Orbit by Ground-Based Lasers. Aeronaut Astronaut 1972;10:74–6.

[320] Hou X, Dong S, Zhou L, Shi D. High Power Electric Generation and WPT Demonstration Mission. 2024 IEEE Wireless Power Technology Conference and Expo (WPTCE), IEEE; 2024, p. 552–6. https://doi.org/10.1109/WPTCE59894.2024.10557417.

[321] ESA - Space-Based Solar Power overview, https://www.esa.int/Enabling_Support/Space_Engineering_Technology/SOLARIS/Space-Based_Solar_Power_overview (accessed February 24, 2025).

[322] Landry MJ, Rupert JW, Mittas A. Photovoltaic array GaAs cells response driven by high power laser diodes. Solar Cells 1990;29:283–301. https://doi.org/10.1016/0379-6787(90)90002-M.

[323] Spillman WB, Crowne DH, Woodward DW. Optically powered and interrogated rotary position sensor for aircraft engine control applications. Opt Lasers Eng 1992;16:105–18. https://doi.org/10.1016/0143-8166(92)90003-P.

[324] Lopez-Cardona JD, Sanchez Montero D, Vazquez C. Smart Remote Nodes Fed by Power Over Fiber in Internet of Things Applications. IEEE Sens J 2019;19:7328–34. https://doi.org/10.1109/JSEN.2019.2915613.

[325] Pellico W, Arroyave MA, Behera B, Cavanna F, Guo F, Heindel A, et al. Power over fiber development for HEP detectors. Nucl Instrum Methods Phys Res A 2024;1069:169880. https://doi.org/10.1016/j.nima.2024.169880.

[326] Rose BH. Monolithic, series connected GaAs photovoltaic power converters for optoelectronic component applications. United States: 1992.

[327] Peña R, Algora C, Matías IR, López-Amo M. Fiber-based 205-mW (27% efficiency) power-delivery system for an all-fiber network with optoelectronic sensor units. Appl Opt 1999;38:2463. https://doi.org/10.1364/AO.38.002463.

[328] Worms K, Klamouris C, Wegh F, Meder L, Volkmer D, Philipps SP, et al. Reliable and lightning-safe monitoring of wind turbine rotor blades using optically powered sensors. Wind Energy 2017;20:345–60. https://doi.org/10.1002/we.2009.

[329] de Nazare FVB, Werneck MM. Hybrid Optoelectronic Sensor for Current and Temperature Monitoring in Overhead Transmission Lines. IEEE Sens J 2012;12:1193–4. https://doi.org/10.1109/JSEN.2011.2163709.

[330] Fakidis J, Helmers H, Haas H. Simultaneous Wireless Data and Power Transfer for a 1-Gb/s GaAs VCSEL and Photovoltaic Link. IEEE Photonics Technology Letters 2020;32:1277–80. https://doi.org/10.1109/LPT.2020.3018960.

[331] Goto K, Nakagawa T, Nakamura O, Kawata S. An implantable power supply with an optically rechargeable lithium battery. IEEE Trans Biomed Eng 2001;48:830–3. https://doi.org/10.1109/10.930908.

[332] Murakawa K, Kobayashi M, Nakamura O, Kawata S. A wireless near-infrared energy system for medical implants. IEEE Engineering in Medicine and Biology Magazine 1999;18:70–2. https://doi.org/10.1109/51.805148.

[333] Mujeeb-U-Rahman M, Adalian D, Chang C-F, Scherer A. Optical power transfer and communication methods for wireless implantable sensing platforms. J Biomed Opt 2015;20:095012. https://doi.org/10.1117/1.JBO.20.9.095012.

[334] Nugent T, Kare J, Bashford D, Erickson C, Alexander J. 12-HOUR HOVER: FLIGHT DEMONSTRATION OF A LASER-POWERED QUADROCOPTER. 2010.

[335] Kim S-M, Choi J, Jung H. Experimental demonstration of underwater optical wireless power transfer using a laser diode. Chinese Optics Letters 2018;16:80101. https://doi.org/10.1364/COL.16.080101.

[336] Jin MH-C, Pierce JM, Lambiotte JC, Fite JD, Marshall JS, Huntley MA. Underwater Free-Space Optical Power Transfer: An Enabling Technology for Remote Underwater Intervention. Day 4 Thu, May 03, 2018, OTC; 2018. https://doi.org/10.4043/28892-MS.

[337] Takahashi R, Hayashi S, Watanabe K, Jikun L, Iida T, Suzuki J, et al. Optical Wireless Power Transmission under Deep Seawater Using GaInP Solar Cells. Energies (Basel) 2024;17:1572. https://doi.org/10.3390/en17071572.

[338] Tai Y, Miyamoto T. Experimental Characterization of High Tolerance to Beam Irradiation Conditions of Light Beam Power Receiving Module for Optical Wireless Power Transmission Equipped with a Fly-Eye Lens System. Energies (Basel) 2022;15:7388. https://doi.org/10.3390/en15197388.

[339] Mohsan SAH, Khan MA, Mazinani A, Alsharif MH, Cho H-S. Enabling Underwater Wireless Power Transfer towards Sixth Generation (6G) Wireless Networks: Opportunities, Recent Advances, and Technical Challenges. J Mar Sci Eng 2022;10:1282. https://doi.org/10.3390/jmse10091282.

[340] Park H-J, Park S, Kim R, Yoo H, Sun H, Yoo D. IoT sensor solution using a PoF module for the environmental monitoring of HVDC-MMC systems. 2019 10th International Conference on Power Electronics and ECCE Asia (ICPE 2019 - ECCE Asia), IEEE; 2019, p. 2834–9. https://doi.org/10.23919/ICPE2019-ECCEAsia42246.2019.8797016.

[341] Diouf C, Quintard V, Ghisa L, Guegan M, Perennou A, Gautier L, et al. Design, Characterization, and Test of a Versatile Single-Mode Power-Over-Fiber and Communication System for Seafloor Observatories. IEEE Journal of Oceanic Engineering 2020;45:656–64. https://doi.org/10.1109/JOE.2018.2876049.

[342] Takeda K, Kawashima N. 100 m Laser Energy Transportation Experiment to a Model Rover to Explore the Ice on the Moon. JOURNAL OF THE JAPAN SOCIETY FOR AERONAUTICAL AND SPACE SCIENCES 2003;51:393–6. https://doi.org/10.2322/jjsass.51.393.

[343] Pradana Putra E, Ker PJ, Lee HJ, Abdullah F, Awang R, Mohd Yusof FA. Optimum operating conditions of a Si-based power over fiber system for high power conversion efficiency at 915 to 976 nm. J Photonics Energy 2024;14. https://doi.org/10.1117/1.JPE.14.048002.

[344] Prajzler V, Zikmund M. Power over fiber system using high-power laser source operating at 1470 nm with maximum power 2.0 W for powering to distance up to 5855 m. Optical Fiber Technology 2024;88:104033. https://doi.org/10.1016/j.yofte.2024.104033.

[345] Yasui T, Ohwaki J, Mino M. A Stable 2-W Supply Optical Powering System. IEEJ Transactions on Electronics, Information and Systems 2002;122:1089–93. https://doi.org/10.1541/ieejeiss1987.122.7_1089.

[346] Lopez Cardona JD, Lallana P, Altuna R, Fresno-Hernandez A, Barreiro X, Vazquez C. Optically Feeding 1.75 W With 100 m MMF in Efficient C-RAN Front-Hauls With Sleep Modes. Journal of Lightwave Technology 2021;39:7948–55. https://doi.org/10.1109/JLT.2021.3078848.

[347] Osório JH, Rosolem JB, Bassan FR, Amrani F, Gérôme F, Benabid F, et al. Hollow-core photonic crystal fibers for Power-over-Fiber systems. Optical Fiber Technology 2022;73:103041. https://doi.org/10.1016/j.yofte.2022.103041.

[348] Matsuura M. Power-Over-Fiber Using Double-Clad Fibers. Journal of Lightwave Technology 2022;40:3187–96. https://doi.org/10.1109/JLT.2022.3164566.

[349] Zhou Y, Guan C, Lv H, Zhang Y, Zhou R, Chu W, et al. Design and Research of Laser Power Converter (LPC) for Passive Optical Fiber Audio Transmission System Terminal. Photonics 2023;10:1257. https://doi.org/10.3390/photonics10111257.

[350] Fafard S, Masson D. Demonstration of Power-over-Fiber with Watts of Output Power Capabilities over Kilometers or at Cryogenic Temperatures. Photonics 2024;11:596. https://doi.org/10.3390/photonics11070596.

[351] Katsuta Y, Miyamoto T. Design and experimental characterization of optical wireless power transmission using GaAs solar cell and series-connected high-power vertical cavity surface emitting laser array. Jpn J Appl Phys 2018;57:08PD01. https://doi.org/10.7567/JJAP.57.08PD01.

[352] Zhou Y, Miyamoto T. 400 mW class high output power from LED-array optical wireless power transmission system for compact IoT. IEICE Electronics Express 2021;18:20200405–20200405. https://doi.org/10.1587/elex.17.20200405.

[353] Zhao M, Miyamoto T. 1 W High Performance LED-Array Based Optical Wireless Power Transmission System for IoT Terminals. Photonics 2022;9:576. https://doi.org/10.3390/photonics9080576.

[354] Zhao M, Miyamoto T. Efficient LED-Array Optical Wireless Power Transmission System for Portable Power Supply and Its Compact Modularization. Photonics 2023;10:824. https://doi.org/10.3390/photonics10070824.

[355] Zhou Y, Miyamoto T. 200 mW-class LED-based optical wireless power transmission for compact IoT. Jpn J Appl Phys 2019;58:SJJC04. https://doi.org/10.7567/1347-4065/ab24b4.

[356] Fakidis J, Videv S, Kucera S, Claussen H, Haas H. Indoor Optical Wireless Power Transfer to Small Cells at Nighttime. Journal of Lightwave Technology 2016;34:3236–58. https://doi.org/10.1109/JLT.2016.2555883.

[357] Wong YL, Shibuya T, Hayashi S, Komazawa Y, Kurooka K, Kikuchi T, et al. Long-Distance Optical Wireless Power Transmission over 100 m using GaInP Solar Cell under 609 nm Laser Irradiation. 31st International Photovoltaic Science and Engineering Conference, PVSEC-31, Online: 2021.

[358] U.S. Naval Research Laboratory. Researchers transmit energy with laser in 'historic' power-beaming demonstration, https://www.nrl.navy.mil/Media/News/Article/2504007/researchers-transmit-energy-with-laser-in-historic-power-beaming-demonstration/ (accessed March 11, 2024).

[359] JAXA - Japan Aerospace Exploration Agency. 日立G1TOWERでの上下方向レーザー伝送実験の実施結果について 2016.

https://www.kenkai.jaxa.jp/research/ssps/pdf/lssps_shiryo.pdf (accessed March 11, 2024).

[360] Ortabasi U, Friedman H. Powersphere: A Photovoltaic Cavity Converter for Wireless Power Transmission using High Power Lasers. 2006 IEEE 4th World Conference on Photovoltaic Energy Conference, IEEE; 2006, p. 126–9. https://doi.org/10.1109/WCPEC.2006.279380.

[361] Smith MD, Brandhorst J, Henry W. Support to a Wireless Power System Design. 2011. https://doi.org/10.21236/ADA564824.